



Published in final edited form as:

J Med Chem. 2019 February 14; 62(3): 1609–1625. doi:10.1021/acs.jmedchem.8b01868.

A Metal-Binding Pharmacophore Library Yields the Discovery of a Glyoxalase 1 Inhibitor

Christian L. Perez¹, Amanda M. Barkley-Levenson², Benjamin L. Dick¹, Peter F. Glatt¹, Yadira Martinez³, Dionicio Siegel³, Jeremiah D. Momper³, Abraham A. Palmer^{2,4,*}, and Seth M. Cohen^{1,*}

¹Department of Chemistry and Biochemistry, University of California San Diego, La Jolla, CA 92093

²Department of Psychiatry, University of California San Diego, La Jolla, CA 92093

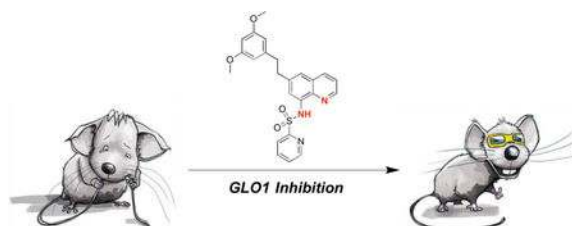
³Skaggs School of Pharmacy and Pharmaceutical Sciences, University of California San Diego, La Jolla, CA 92093

⁴Institute for Genomic Medicine, University of California San Diego, La Jolla, CA 92093

Abstract

Anxiety and depression are common, highly comorbid psychiatric diseases that account for a large proportion of worldwide medical disability. Glyoxalase 1 (GLO1) has been identified as a possible target for the treatment of anxiety and depression. GLO1 is a Zn²⁺-dependent enzyme that isomerizes a hemithioacetal, formed from glutathione and methylglyoxal, to a lactic acid thioester. To develop active inhibitors of GLO1, fragment-based drug discovery (FBDD) was used to identify fragments that could serve as core scaffolds for lead development. After screening a focused library of metal-binding pharmacophores, 8-(methylsulfonylamino)quinoline (**8-MSQ**) was identified as a hit. Through computational modeling and synthetic elaboration, a potent GLO1 inhibitor was developed with a novel sulfonamide core pharmacophore. A lead compound was demonstrated to penetrate the blood-brain barrier, elevate levels of methylglyoxal in the brain, and reduce depression-like behavior in mice. These findings provide the basis for GLO1 inhibitors to treat depression and related psychiatric illnesses.

Graphical Abstract



* aap@ucsd.edu, scohen@ucsd.edu.

Supporting Information

Schemes S1-S2, Figures S1-S5, PDB files of modeled structures, and Table S1 that contains information on compound purity and Molecular Formula Strings.

INTRODUCTION

Anxiety and depression are the two most common psychiatric disorders in the U.S. and affect approximately one-in-five adults at some point in their lifetime. Depression is the leading cause of worldwide disability and anxiety disorders, which are highly comorbid with depression, are the sixth leading cause of worldwide disability.¹ There are already several drugs approved by the U.S. Food and Drug Administration for the treatment of both anxiety and depression; however, these drugs have limitations. Anxiolytic drugs produce sedating side effects and have significant abuse liability. Antidepressant drugs are not effective in all patients, take weeks to produce therapeutic effects, and produce side effects that limit their use.² Therefore, there is an urgent need for developing better therapeutics.

Glyoxalase 1 (GLO1) is a cytosolic Zn²⁺-dependent isomerase that is part of the glyoxalase system, a pathway involved in the detoxification of α -oxoaldehydes.³⁻⁶ Methylglyoxal (MG) is a reactive metabolite generated via the degradation of glycolytic intermediates and is capable of forming covalent adducts with proteins and nucleotides that result in advanced glycation end (AGE) products, reactive-oxygen species (ROS), and apoptosis.⁶⁻⁹ GLO1 catalyzes the isomerization of a hemithioacetal formed from a spontaneous reaction between glutathione (GSH) and MG. The resulting thioester is then converted by glyoxalase 2 (GLO2) to a less reactive metabolite, D-lactate, and in this capacity helps deplete MG levels.^{4,10} Due to the role in AGE formation and cytotoxicity, GLO1 inhibitors have been investigated as potential oncogenic therapeutics but have not yet found clinical success.^{11,12}

Recent studies using both genetic and pharmacological techniques have implicated GLO1 in numerous behaviors, including several that are relevant to anxiety and depression.¹³⁻¹⁷ MG has been shown to be a competitive partial GABA-A receptor agonist.¹⁵ Taken together, these data suggest that inhibition of GLO1 can cause an accumulation of MG, leading to activation of GABA-A receptors, and thus producing potentially therapeutic changes in behavior.

Several natural products and natural product derivatives that inhibit GLO1 have been described.¹⁸ Glutathione-based inhibitors were among the first GLO1 inhibitors reported with a compound containing a hydroxamic acid MBP (**AHC-GSH**, Figure 1) being the first tight binding inhibitor to be reported.¹⁹ These glutathione mimics have poor membrane permeability and need to be administered as prodrugs (i.e. esters), in order to achieve membrane penetration.¹¹ **AHC-GSH** prodrug analogs have demonstrated some efficacy in vivo, but suffer from rapid clearance (in esterase deficient mice) and have a narrow therapeutic window.²⁰ Both the hydroxamic acid MBP and glutathione origins of **AHC-GSH**, and its analogs, make these molecules unsuitable as viable drug candidates. A second class of reported inhibitors are flavonoids and flavonoid analogs which tend to coordinate the catalytic metal of GLO1 via a catechol moiety.²¹⁻²⁷ Methyl gerfelin (**M-GFN**) was reported as a potent inhibitor of GLO1 within the flavonoid class (Figure 1).²⁶ Lastly, a *N*-hydroxypyridinone based inhibitor (**Chugai-3d**, Figure 1) reported by Chugai Pharmaceuticals shows an excellent IC₅₀ value of 11 nM.²⁸ However, to the best of our knowledge, in vivo studies or clinical trials have not been reported with **Chugai-3d**. The majority of these inhibitors have been designed and investigated for oncogenic indications

and may not be suitable candidates for targets within the central nervous system (CNS). Therefore, we sought to develop a novel GLO1 inhibitor that could penetrate the blood-brain barrier (BBB) and inhibit GLO1.

A fragment-based drug discovery (FBDD) approach was used to identify a novel GLO1 inhibitor. The use of FBDD for the discovery of biologically active compounds has become increasingly important.²⁹ This strategy consists of generating small libraries of molecular fragments and screening them against the target of interest. For metalloenzyme targets such as GLO1, FBDD libraries have been designed consisting of metal-binding pharmacophores (MBPs), where “hits” from these libraries can be elaborated into lead compounds. MBPs are small molecules that have a set of donor atoms that are capable of coordinating to the active site metal ion of metalloenzymes.³⁰ Here, we report the discovery, design, synthesis, and evaluation of a novel class of GLO1 inhibitors obtained from metalloenzyme-targeted FBDD. An *in vitro* inhibition assay and computational molecular modeling were utilized to develop structure-activity relationship (SAR). Further biological *in vivo* assessment of a lead compound in mice demonstrated that it penetrates the BBB, increases MG levels in the brain (indicating target engagement of GLO1 *in vivo*), and results in changes in behavioral phenotypes in mice comparable to other GLO1 inhibitors and prototypical tricyclic and serotonin reuptake inhibitors (SRIs) antidepressants. Our findings lend further support to the potential of GLO1 inhibitors to provide a novel therapeutic strategy for the treatment of depression and anxiety.

RESULTS

Screening of the MBP Library.

For the development of metalloenzyme inhibitors, an MBP library has been previously reported for producing hits.^{31–34} To identify MBPs that could serve as scaffolds for GLO1 inhibitors, a chemical library containing ~240 MBP fragments was screened against GLO1 utilizing a previously reported enzyme-based assay adapted for a 96-well plate format.³⁵ The assay was performed in a 96-well plate format using a colorimetric output that measures the isomerization of a hemithioacetal to a lactic acid thioester. The MBP library was initially screened at a fragment concentration of 200 μM yielding >50 unique hits displaying >50% inhibition. A second screening at a lower concentration of 50 μM produced 25 distinct hits. From this second screening, 8-(methylsulfonylamino)quinoline (**8-MSQ**) showed essentially complete inhibition and was subsequently shown to have an IC_{50} value of $18.5 \pm 0.5 \mu\text{M}$ (Table 1). Because of the particularly strong activity of **8-MSQ**, the fragment was chosen for lead development.

The lead fragment **8-MSQ** has been previously reported as an MBP, as well as a receptor unit in molecular sensors for Zn^{2+} .^{36–39} Based on these previous reports, we predicted that **8-MSQ** would bind the catalytic Zn^{2+} ion of GLO1 in a bidentate fashion through the endocyclic nitrogen and exocyclic sulfonamide-nitrogen donor atoms (Figure 1). To validate this hypothesis, a series of compounds were synthesized wherein the metal-coordinating atoms were substituted or replaced (Table 1). Compounds **2** and **3** place the coordinating endocyclic nitrogen at different positions within the quinoline ring. Additionally, **4** replaces the sulfonamide with a sulfonate ester, while **5** replaces the sulfonamide with an amide.

Lastly, compound **6** incorporates a reverse sulfonamide functional group. As highlighted by the data in Table 1, compounds **2-6** all showed a complete loss of activity ($IC_{50} > 200 \mu M$) against GLO1, further suggesting the importance of the specific bidentate binding of **8-MSQ** through the nitrogen pair of donor atoms.

8-MSQ Derivatives and Rudimentary SAR.

The core quinoline scaffold of compound **8-MSQ** has several positions amenable for derivatization. In this study, the optimal point(s) of attachment were determined based on computational modeling and structural studies. Modeling studies were performed using the Molecular Operating Environment (MOE) software suite (see ESI for details), which can account for flexible protein domains and can assist in pharmacophore modeling and SAR studies. Using a crystal structure of GLO1 (PDB 3VW9)²⁸ an inhibitor pharmacophore model was generated. The crystal structure selected has a resolution of 1.47 Å and has the **Chugai-3d** inhibitor bound (Figure 1) to the active site of GLO1. Structural analysis of this crystal structure revealed a Zn^{2+} metal center and two distinct pockets within the GLO1 active site: a hydrophobic and a GSH-binding pocket. The hydrophobic pocket consists of residues Cys60, Phe62, Ile88, Met179, Leu182, and Met183. The GSH-binding pocket consists of Phe67, Leu69, Met157, Phe162, as well as the conserved water network (Figure 2). The catalytic Zn^{2+} has an octahedral geometry and is coordinated by Gln33, Glu99, Glu172, and His126, with the 5th and 6th coordination sites occupied by the *O,O* donor atoms of the **Chugai-3d** compound (Figure 2). The **Chugai-3d** binding affinity is attributed to significant contacts with both the hydrophobic and GSH-binding pockets, as well as the water network. The 6-phenyl moiety of **Chugai-3d** occupies the hydrophobic pocket and engages in edge-to-face interactions with Phe62 and additional hydrophobic contacts with Met179 and Met183 (Figure 2). The 7-azaindole forms an edge-to-face interaction with Phe67 and a hydrophobic contact with Leu69 (Figure 2). Additionally, the 7-azaindole nitrogen atom is directly facing a water molecule and engaging in a hydrogen bond. The binding conformation and the critical contacts made by **Chugai-3d** with GLO1 allowed for the development of a crude pharmacophore model to guide inhibitor design derived from **8-MSQ**.

A binding model for **8-MSQ** was obtained through docking of the fragment into the GLO1 active site and superimposing the coordinating atoms (*N,N*) of **8-MSQ** with those of the bound **Chugai-3d** inhibitor. The superposition of **8-MSQ** generated a probable binding mode in which the endocyclic nitrogen of the quinoline ring is bound at the equatorial site of the metal center and the exocyclic nitrogen of the sulfonamide functional group is bound axial of the metal center (Figure 2). The docked pose was well tolerated with no major clash predicted between the fragment and the receptor. Another mode of binding can be modeled by alternating the position of the donor set; however, modeling suggested that this alternate binding pose is likely to cause significant steric clashes with the GLO1 active site (Figure S1). Therefore, initial assessment of these two poses pointed towards the pose shown in Figure 2 as the most likely mode of binding.

To determine whether the computational model developed in Figure 2 was predictive, a small set of compounds was synthesized to evaluate the model. Compounds **7-9** were

synthesized in a straightforward, one-step manner starting with 8-aminoquinoline or 2-methyl-8-aminoquinoline and combining with the corresponding sulfonyl chloride (Scheme S1). Enzyme-based assay evaluation of compound **7** yielded a poorer IC₅₀ value (~2-fold loss of affinity compared to **8-MSQ**) due simply to the introduction of a methyl substituent (Table 1). As demonstrated in Figure 2 the introduction of a methyl group would generate a steric clash with Gln33; therefore, this loss of activity is consistent with the computational modeling. Compound **8** incorporates a phenyl at the 8-sulfonamide position and results in a 2-fold improvement in inhibition, which also validates the computational model, where the added phenyl group can be accommodated in the glutathione binding pocket (Figure S2). From this docked pose, compound **8** forms a hydrogen bond between the sulfone and a water molecule (W1). An additional edge to face interaction between the phenyl moiety and Phe67 (~4.5 Å) and a hydrophobic interaction between the phenyl group and Leu69 (~4.2 Å) are predicted. Compound **9** incorporates both a 2-methyl and an 8-phenylsulfonamide which results in a slight increase in inhibition relative to **8-MSQ**, but worse activity when compared with **8** (Table 1). Taken together these results support the predicted mode of binding for **8-MSQ** (Figure 2) and indicate functional groups at the sulfonamide moiety are well tolerated to fit in the GSH-binding pocket. Using a fixed Zn²⁺-coordination geometry for **8-MSQ**, the SAR around the fragment was explored by making independent substitutions at the sulfonamide 8-position.

8-Sulfonamidequinoline Analogs.

Compound **8** demonstrated that a phenyl group was well tolerated within the GSH-binding pocket (Table 1). Therefore, different substituents were explored to find a more optimal group to enhance interactions with this pocket. A diverse range of aliphatic, functionalized phenyl, and heterocyclic functional groups were probed at the 8-position. Preparation and screening of several derivatives (Table 2) demonstrated that aliphatic substituents (**10-13**) were not tolerated and resulted in poorer inhibition than **8-MSQ**. However, compounds that incorporated heterocyclic or aromatic rings, such as thiophene, furan, phenyl, and pyridine (**14-15**, **18-19**, **21-24**, **27-30**) gave modest improvements in activity, with compound **23** showing the largest (~14-fold) improvement. Three compounds incorporated fused-ring systems (**31-33**) also showed modest improvements in activity. Alternatively, extending the linker between the sulfonamide functional group and the phenyl substituent (**34-36**) did not seem to change inhibition significantly. Interestingly, compounds **17** and **20** that incorporate a methoxy or nitrile at the ortho position (relative to sulfonamide) were not tolerated; modeling of these compounds within the active site predicted a significant clash with a W1 and limited intramolecular rotation. Ultimately, compound **23** (Table 2, IC₅₀ value 1.3 μM) was the most active derivative from this group by making the best interactions within the GSH-binding pocket. Similarly to compound **8**, the 2-pyridinyl group forms an edge-to-face interaction with Phe67 and a hydrophobic contact with Leu69 (Figure S3). Additionally, the 2-pyridinyl nitrogen is directly facing W1 and engaging in a hydrogen bond.

5-Aryl/Cyclic-8-(Methylsulfonylamino)quinoline Derivatives.

A second set of compounds was pursued to identify substituents that interact within the hydrophobic pocket (Figure 2). This series of compounds complements the study exploring

the GSH-binding pocket and were later merged to find a lead compound with favorable substituents at each position (vide infra). For the synthesis of this series the procedure shown in Scheme 1 was used. First, 5-bromoquinoline was selectively nitrated at the 8-position yielding 5-bromo-8-nitroquinoline. Then, this intermediate was utilized to attach aryl or amine substituents at the 5-position via Suzuki or Buchwald-Hartwig coupling reactions. The products of the coupling reaction were then reduced via palladium on carbon under a hydrogen atmosphere or through the use of sodium dithionite resulting in the free amine compound. Lastly, the amine was coupled with methylsulfonyl chloride under basic conditions. A set of 10 compounds was synthesized, with diverse functional groups at the 5-position. Evaluation of these compounds against GLO1 showed that polar (**38**, **39**) or non-aromatic (**45**, **46**) groups were not well tolerated (Table 3). Some compounds containing hydrophobic phenyl substituents resulted in modest (~3-fold) improvements in inhibition relative to **8-MSQ** (**37**, **40-44**, Table 3).

Merged Compounds.

Using the best performing functional groups identified for both the 5- and 8-positions, a fragment merging strategy was employed to produce a series of compounds. The functionality at the 8-position (2-pyridinylsulfonamide) was maintained throughout this series, with structural variation at the 5-position. Additionally, a handful of compounds were synthesized with substituents at the 6-position, instead of the 5-position, to provide more SAR information. Synthesis of these compounds generally followed Scheme 1 where the intermediate, 5-bromo-8-nitroquinoline or 6-bromo-8-nitroquinoline (Scheme S2), was coupled to aryl groups, amines, or alkynes via Suzuki, Buchwald, or Sonogashira methods. Compounds containing alkynes were reduced to alkanes in a one-pot reduction of the alkyne and nitro with palladium on carbon and hydrogen. Compounds containing phenyl, chlorophenyl, and fluorophenyl substituents (**47-50**, **53-54**, **57**, and **59**) were primarily explored (Table 4). Additionally, compounds **51-52**, **55**, and **60** were inspired by flavonoid GLO1 inhibitors previously reported.²¹⁻²⁷ These efforts yielded a rather flat SAR, but with several inhibitors showing IC₅₀ values of <1 μM, with **49** and **60** demonstrating the best inhibition with an IC₅₀ value of 370 and 460 nM, respectively (Table 4). A model for the binding of these compounds (specifically compound **47**) shows how the 5- and 8-substituents occupy the hydrophobic and GSH binding pockets in GLO1 (Figure S4).

Behavioral Testing.

Preliminary behavioral testing in mice used compound **48**, which was found to be visibly toxic at intraperitoneal (i.p.) doses of 50 mg/kg and higher. Compound **60** was chosen as an alternative, and observational assessment of toxicity showed no adverse responses with doses up to 100 mg/kg i.p. To evaluate whether **60** showed an antidepressant-like behavioral profile, we employed the forced swim test (FST), which is an assay that is widely used to screen compounds for antidepressant efficacy.⁴⁰ We also used the open field test in an effort to identify unexpected changes in locomotor behavior following drug treatment, which might confound our interpretation of the FST. Mice were weighed and given an i.p. injection with either 12.5 mg/kg of the GLO1 inhibitor **60** or vehicle (8% DMSO, 18% Tween, 80% H₂O) and were returned to the home cage. Ninety minutes after injection, mice were placed

in the open field apparatus for 30 min. Immediately after open field testing, mice were transported to a different procedure room and given a 6 min FST. At the end of testing, mice were returned to the colony. Approximately three weeks later, mice were again weighed and given an i.p. injection with either 12.5 mg/kg of the GLO1 inhibitor **60** or vehicle. After two hours, mice were given another 6 min FST. Drug treatment order was counterbalanced relative to the first day of testing, such that each mouse receive vehicle on one day and **60** on the other. Drug-treated animals showed a reduction in percent immobility as compared to vehicle-treated animals (Figure 3). This is consistent with an antidepressant effect for **60**, and is similar to previously reported results for other GLO1 inhibitors.⁴¹

Brain Exposure and Effect on MG Brain Levels.

Given the behavioral results, we used a separate cohort of mice to examine brain levels of **60** and to establish target engagement by measuring brain MG concentrations. Following 12.5 mg/kg i.p. doses of **60**, median brain levels of the compound at 30, 60, 120, and 240 min were 2.1, 14.4, 6.0, and 2.2 ng/mg of wet weight brain tissue ($n=3$ per time point). At 25 mg/kg i.p., median brain levels at 30, 60, 120, and 240 min were 0.4, 6.7, 18.9, and 8.3 ng/mg of wet weight brain tissue ($n=3$ per time point). MG levels in brain between 30 and 240 min post-dose were increased approximately 11-fold and 13-fold in mice treated with 12.5 mg/kg and 25 mg/kg of **60**, respectively, as compared to vehicle-treated mice (MG per mg brain tissue in **60** 12.5 mg/kg and 25 mg/kg groups 11.8 ± 4.1 and 14.1 ± 3.1 , respectively, versus 1.1 ± 0.3 in vehicle-treated mice). Collectively, these data suggest on-target engagement of GLO1 by **60**, resulting in accumulation of MG, and the observed behavioral effects in mice (vide supra).

DISCUSSION

In order to discover a GLO1 inhibitor, a FBDD approach using a ~240-component library of MBPs was utilized in two independent screens at two different concentrations, 200 μ M and 50 μ M. Screening led to the identification of the highly active **8-MSQ** fragment that was determined to have an IC_{50} value of 18.5 μ M. Upon identifying **8-MSQ** as the lead fragment, several analogs were evaluated to determine whether metal binding was the mechanism of GLO1 inhibition. The SAR obtained from compounds **2-6** (Table 1) strongly suggests that bidentate metal coordination is necessary for the observed inhibitory activity of **8-MSQ**. The identification of **8-MSQ** prompted the development of a computational model that identified the 5- and 8-positions as suitable positions for derivatization, fragment growth, and lead inhibitor development. A strategy was then implemented in which the substituent off each position was explored independently.

Initial synthetic efforts were confined to substituents exploring modifications to the 8-position, which is situated within the GSH-binding pocket of the GLO1 active site. A variety of substituents were explored via a sulfonamide linkage as demonstrated in Table 2. The introduction of non-aromatic alkane chains led to loss of inhibition (**10-13**). However, compounds that incorporated heterocyclic or aromatic rings, such as thiophene, furan, phenyl, and pyridine (**14-15**, **18-19**, **21-22**, **24**, **27-30**) all improved activity modestly. Three compounds incorporated fused-ring systems (**31-33**) and were among the best inhibitors of

this subset of molecules. Alternatively, extending the linker between the sulfonamide functional group and the phenyl substituent (**34-36**) did not change inhibition significantly. Introduction of a 2-pyridyl moiety (**23**) yielded the best inhibition against GLO1 and computational modeling suggested the nitrogen of the 2-pyridyl moiety is engaged in a hydrogen bond with an active site water (Figure S3).

Additional synthetic efforts were made to explore the GLO1 active site hydrophobic pocket. A small library of inhibitors with functionalization at the 5-position were prepared. Generally, only hydrophobic aromatic functional groups were tolerated (**37, 40-44**), while compounds containing polar heterocyclic or non-aromatic substituents (**38-39, 45-46**) demonstrated significant loss of inhibition (Table 3). Combining preferred substituents on the 5- and 8-positions using a fragment-merge strategy gave a series of lead compounds (Table 4). Although the SAR of these lead compounds was somewhat flat, several compounds were identified with IC₅₀ values in the range of ~370–800 nM, representing a ~40-fold improvement in activity when compared to the parent fragment **8-MSQ**. These lead compounds are comparably active to the GLO1 inhibitor methyl gerfelin, but are substantially more druglike (e.g., lacking PAINS such as the catechol group in methyl gerfelin).⁴²

In an effort to evaluate behavioral effects of **60**, in vivo studies were performed in mice. We confirmed that **60** reduced immobility in the FST (Figure 3), which is consistent with prior observations for two other GLO1 inhibitors: *S*-bromobenzylglutathione cyclopentyl diester (pBBG) and methyl gerfelin.⁴¹ Importantly, the effects on the FST were not accompanied by changes in general locomotor activity, which can confound the interpretation of the FST.⁴⁰ We also assessed levels of **60** in brain over the time course relevant to our behavioral studies. Brain exposure of **60** was similar to that observed with fluoxetine (a prototypical selective serotonin reuptake inhibitor) in rodents⁴³ and was associated with a >10-fold increase in brain MG levels (ng/mg of brain tissue) compared to vehicle-treated mice, indicating target engagement. Taken together, these results show that **60** elevated brain MG levels and produced behavioral changes that are consistent with antidepressant effects. Although not directly tested in these studies, our prior studies showed that the behavioral effects of GLO1 inhibitors occurred more rapidly than conventional antidepressants (e.g., fluoxetine) and could be observed using both acute and chronic models; it is likely that the same would be true of **60**.⁴¹ Our working model suggests that the effects of MG are mediated by its action as an endogenously produced competitive partial agonist at GABA-A receptors,^{14,15,44} however, a recent study has suggested an alternative mechanism, namely that MG may also exert antidepressant effects by direct activation of TrkB receptors.⁴⁵

EXPERIMENTAL

General.

All reagents and solvents were obtained from commercial sources and used without further purification. Microwave reactions were performed in 10 or 35 mL microwave reaction vials using a CEM Discover S reactor. Column chromatography was performed using a Teledyne ISCO CombiFlash Rf system with prepacked silica cartridges or High Performance Gold

C18 columns. $^1\text{H}/^{13}\text{C}$ NMR spectra were recorded at ambient temperature on a 400 or 500 Varian FT-NMR instrument located in the Department of Chemistry and Biochemistry at the U.C. San Diego. Mass spectra were obtained from the Molecular Mass Spectrometry Facility (MMSF) in the Department of Chemistry and Biochemistry at the University of California, San Diego. The purity of all compounds used in assays was determined to be $\geq 95\%$ by high performance liquid chromatography (HPLC) analysis (Table S1, Figure S5) using an Agilent 6230 Accurate-Mass LC-TOFMS from the MMSF at U.C. San Diego.

***N*-(Quinolin-8-yl)methanesulfonamide (8-MSQ).**

To a solution of 8-aminoquinoline (0.1 g, 0.7 mmol) in pyridine (3 mL), methanesulfonyl chloride (0.16 mL, 2.1 mmol) was added. The mixture was stirred at room temperature for 12–15 h. After stirring, H_2O (50 mL) was added to the reaction mixture and the solution was extracted with EtOAc (3 \times 50 mL). The combined organic layers were dried over MgSO_4 , filtered, and concentrated via rotary evaporation. The resulting crude oil was purified via silica gel chromatography eluting a gradient of 0–80% EtOAc in hexanes. The product was isolated as an off-white solid. Yield = 0.085 g (55%). ^1H NMR (400 MHz, CDCl_3): δ 8.93 (br, 1H), 8.83 (dd, $J_1 = 4.4$ Hz, $J_2 = 2$ Hz, 1H), 8.20 (dd, $J_1 = 8.4$ Hz, $J_2 = 1.6$ Hz, 1H), 7.87 (dd, $J_1 = 7.2$ Hz, $J_2 = 1.6$ Hz, 1H), 7.58–7.48 (m, 3H), 3.03 (s, 3H). ESI-MS(+): m/z 223.08 $[\text{M}+\text{H}]^+$, 245.04 $[\text{M}+\text{Na}]^+$.

***N*-(Isoquinolin-8-yl)methanesulfonamide (2).**

To a solution of isoquinolin-8-amine (0.2 g, 1.38 mmol) in pyridine (3 mL), methanesulfonyl chloride (0.161 mL, 2.08 mmol) was added, and the mixture was allowed to stir at room temperature for 12–15 h. After stirring, H_2O (50 mL) was added to the reaction mixture and the solution was extracted with EtOAc (3 \times 50 mL). The combined organic layers were dried over MgSO_4 , filtered, and concentrated via rotary evaporation. The resulting crude oil was purified via silica gel chromatography eluting a gradient of 0–20% MeOH in CH_2Cl_2 . Yield = 0.161 g (52%). ^1H NMR (400 MHz, $\text{DMSO}-d_6$): δ 10.75 (br, 1H), 9.92 (s, 1H), 8.70 (d, $J = 6.4$ Hz, 1H), 8.47 (d, $J = 6.4$ Hz, 1H), 8.18–8.12 (m, 2H), 7.93 (d, $J = 6.8$ Hz, 1H), 3.19 (s, 3H). ESI-MS(+): m/z 223.08 $[\text{M}+\text{H}]^+$.

***N*-(Quinolin-5-yl)methanesulfonamide (3).**

To a solution of quinoli-5-amine (0.2 g, 1.38 mmol) in pyridine (3 mL), methanesulfonyl chloride (0.161 mL, 2.08 mmol) was added, and the mixture was allowed to stir at room temperature for 12–15 h. After stirring, H_2O (50 mL) was added to the reaction mixture and the solution was extracted with EtOAc (3 \times 50 mL). The combined organic layers were dried over MgSO_4 , filtered, and concentrated via rotary evaporation. The resulting crude oil was purified via silica gel chromatography eluting a gradient of 0–16% MeOH in CH_2Cl_2 . Yield = 0.11 g (38%). ^1H NMR (400 MHz, CDCl_3): δ 8.41 (dd, $J_1 = 8.4$ Hz, $J_2 = 1.6$ Hz, 1H), 8.29 (d, $J = 8.4$ Hz, 1H), 7.81 (t, $J = 8.4$ Hz, 1H), 7.64 (dd, $J_1 = 8.4$ Hz, $J_2 = 1.6$ Hz, 1H), 7.59 (dd, $J_1 = 8.4$ Hz, $J_2 = 4.0$ Hz, 1H), 3.51 (s, 3H). ESI-MS(+): m/z 223.11 $[\text{M}+\text{H}]^+$.

Quinolin-8-yl methanesulfonate (4).

To a solution of 8-hydroxyquinoline (0.2 g, 1.38 mmol) in pyridine (3 mL), methanesulfonyl chloride (0.322 mL, 4.13 mmol) was added, and the mixture was allowed to stir at room temperature for 12–15 h. After stirring, H₂O (50 mL) was added to the reaction mixture and the solution was extracted with EtOAc (3×50 mL). The combined organic layers were dried over MgSO₄, filtered, and concentrated via rotary evaporation. The resulting crude oil was purified via silica gel chromatography eluting a gradient of 0–70% EtOAc in hexanes. Yield = 0.085 g (34%). ¹H NMR (400 MHz, CDCl₃): δ 8.91 (dd, *J*₁ = 4.0 Hz, *J*₂ = 1.6 Hz, 1H), 8.15 (dd, *J*₁ = 8.4 Hz, *J*₂ = 1.2 Hz, 1H), 7.73 (d, *J* = 8.0 Hz, 1H), 7.67 (d, *J* = 8.0 Hz, 1H), 7.50 (t, *J* = 8.0 Hz, 1H), 7.43 (dd, *J*₁ = 8.4 Hz, *J*₂ = 4.4 Hz, 1H), 3.40 (s, 3H). ESI-MS(+): *m/z* 224.25 [M+H]⁺.

N-(Quinolin-8-yl)acetamide (5).

To a solution of 8-aminoquinoline (0.2 g, 1.38 mmol) in pyridine (3 mL), acetyl chloride (0.148 mL, 2.08 mmol) was added, and the mixture was allowed to stir at room temperature for 12–15 h. After stirring, H₂O (50 mL) was added to the reaction mixture and the solution was extracted with EtOAc (3×50 mL). The combined organic layers were dried over MgSO₄, filtered, and concentrated via rotary evaporation. The resulting crude oil was purified via silica gel chromatography eluting a gradient of 0–60% EtOAc in hexanes. Yield = 0.076 g (32%). ¹H NMR (400 MHz, CDCl₃): δ 9.78 (br, 1H), 8.81 (dd, *J*₁ = 4.0 Hz, *J*₂ = 1.6 Hz, 1H), 8.77 (dd, *J*₁ = 8.0 Hz, *J*₂ = 1.6 Hz, 1H), 8.17 (dd, *J*₁ = 8.0 Hz, *J*₂ = 1.6 Hz, 1H), 7.55–7.48 (m, 2H), 7.47 (dd, *J*₁ = 8 Hz, *J*₂ = 5 Hz, 1H), 2.35 (s, 3H). ESI-MS(+): *m/z* 187.23 [M+H]⁺.

N-Methylquinoline-8-sulfonamide (6).

To a solution of quinoline-8-sulfonyl chloride (0.2 g, 0.88 mmol) in pyridine (3 mL), methylamine (2M THF solution, 1.31 mL, 0.082 mmol) was added, and allowed to stir at room temperature for 12–15 h. After stirring, H₂O (50 mL) was added to the reaction mixture and the solution was extracted with EtOAc (3×50 mL). The combined organic layers were dried over MgSO₄, filtered, and concentrated via rotary evaporation. The resulting crude oil was purified via silica gel chromatography eluting a gradient of 0–55% EtOAc in hexanes. Yield = 0.110 g (43%). ¹H NMR (400 MHz, CDCl₃): δ 9.03 (d, *J* = 4.0 Hz, 1H), 8.47 (d, *J* = 8.0 Hz, 1H), 8.31 (d, *J* = 8.0 Hz, 1H), 8.09 (d, *J* = 8.0 Hz, 1H), 7.70 (t, *J* = 8.0 Hz, 1H), 7.59 (dd, *J*₁ = 8.0 Hz, *J*₂ = 4.0 Hz, 1H), 6.26 (br, 1H), 2.59 (d, *J* = 5.6 Hz, 3H). ESI-MS(+): *m/z* 223.15 [M+H]⁺.

N-(2-Methylquinolin-8-yl)methanesulfonamide (7).

To a solution of 2-methylquinolin-8-amine (0.2 g, 1.26 mmol) in pyridine (3 mL) methanesulfonyl chloride (0.296 mL, 3.79 mmol) was added, and the mixture was allowed to stir at room temperature for 15 h. After stirring, H₂O (50 mL) was added to the reaction mixture and the solution was extracted with EtOAc (3×50 mL). The combined organic layers were dried over MgSO₄, filtered, and concentrated via rotary evaporation. The resulting crude oil was purified via silica gel chromatography eluting 0–10% MeOH in CH₂Cl₂. The desired product was isolated as a dark brown solid. Yield = 0.191 g (64%). ¹H NMR

(DMSO- d_6 , 400 MHz) δ 9.17 (br, 1H), 8.29 (d, J = 8.4 Hz, 1H), 7.67 (m, 2H), 7.51 (m, 2H), 3.15 (s, 3H), 2.70 (s, 3H). ESI-MS(+): m/z 237.07 [M+H]⁺, 258.98 [M+Na]⁺.

Protocol for Sulfonamide Coupling Method A —To a solution of 8-aminoquinoline (0.1 g, 0.69 mmol) in pyridine (3 mL) the corresponding sulfonyl chloride was added, and the mixture was allowed to stir at room temperature for 12–15 h. To the resulting mixture was added H₂O (50 mL) and then the solution was extracted with EtOAc (3×50 mL). The combined organic layers were dried over MgSO₄, then filtered, and concentrated via rotary evaporation. The resulting crude oil was purified via silica gel chromatography eluting a gradient of EtOAc in hexanes.

Protocol for Sulfonamide Coupling Method B —To a solution of 8-aminoquinoline (0.1 g, 0.69 mmol) in pyridine (3 mL) the corresponding sulfonyl chloride (1.04 mmol) was added. The clear solution was heated in a microwave reactor at 130 °C for 3 min (Power = 300W). The solution was then poured into H₂O (12 mL) causing the product to precipitate, which was then isolated via filtration, and rinsed with water. If no precipitate was formed, the aqueous phase was extracted CH₂Cl₂ (2×50mL). The combined organic layers were dried over MgSO₄, filtered, and evaporated in vacuo to obtain a solid when co-evaporated with Et₂O.

***N*-(Quinolin-8-yl)benzenesulfonamide (8).**

Synthesized utilizing Sulfonamide Coupling method B. Isolated as white solid. Yield = 0.179 g (91%). ¹H NMR (CDCl₃, 400 MHz) δ 9.25 (br, 1H), 8.76 (d, J = 4.4 Hz, 1H), 8.10 (d, J = 8.8 Hz, 1H), 7.91 (d, J = 8.0 Hz, 2H), 7.82 (dd, J_1 = 6.4 Hz, J_2 = 2.4 Hz, 1H), 7.41 (m, 6H). ESI-MS(+): m/z 285.03 [M+H]⁺.

***N*-(2-Methylquinolin-8-yl)benzenesulfonamide (9).**

To a solution of 2-methylquinolin-8-amine (0.2 g, 1.26 mmol) in pyridine (3 mL) benzenesulfonyl chloride (0.486 mL, 3.79 mmol) was added, and the mixture was allowed to stir at room temperature for 15 h. After stirring, H₂O (50 mL) was added to the reaction mixture and the solution was extracted with EtOAc (3×50 mL). The combined organic layers were dried over MgSO₄, filtered, and concentrated via rotary evaporation. The resulting crude oil was purified via silica gel chromatography eluting 0–10% MeOH in CH₂Cl₂. The desired product was isolated as a light brown solid. Yield = 0.247 g (66%). ¹H NMR (DMSO- d_6 , 400 MHz) δ 9.76 (br, 1H), 8.18 (d, J = 8.4 Hz, 1H), 7.89 (m, 2H), 7.62–7.39 (m, 7H), 2.63 (s, 3H). ESI-MS(+): m/z 299.11 [M+H]⁺, 321.05 [M+Na]⁺.

***N*-(Quinolin-8-yl)cyclopropanesulfonamide (10).**

Synthesized utilizing Sulfonamide Coupling method A using 1.5 equiv of sulfonyl chloride. Purified with a gradient of 0–30% EtOAc in hexanes. Isolated as white solid. Yield = 0.080 g (45%). ¹H NMR (CDCl₃, 400 MHz) δ 8.92 (br, 1H), 8.83 (dd, J_1 = 4.0 Hz, J_2 = 1.6 Hz, 1H), 8.19 (dd, J_1 = 8.4 Hz, J_2 = 1.6 Hz, 1H), 7.92 (dd, J_1 = 7.2 Hz, J_2 = 1.6 Hz, 1H), 7.57–7.47 (m, 3H), 2.57 (m, 1H), 1.29 (m, 2H), 0.90 (m, 2H). ESI-MS(+): m/z 249.14 [M+H]⁺.

***N*-(Quinolin-8-yl)propane-2-sulfonamide (11).**

Synthesized utilizing Sulfonamide Coupling method A using 3.3 equiv of sulfonyl chloride. Purified with a gradient of 0–40% EtOAc in hexanes. Isolated as tan solid. Yield = 0.040 g (23%). ¹H NMR (400 MHz, CDCl₃): δ 8.86 (br, 1H), 8.82 (dd, *J*₁ = 4.4 Hz, *J*₂ = 2.0 Hz, 1H), 8.18 (dd, *J*₁ = 8.4 Hz, *J*₂ = 1.6 Hz, 1H), 7.90 (dd, *J*₁ = 7.6 Hz, *J*₂ = 2.0 Hz, 1H), 7.54 (m, 3H), 3.37 (sept, *J* = 6.8 Hz, 1H), 1.38 (s, 1H), 1.37 (s, 3H). ESI-MS(+): *m/z* 251.09 [M+H]⁺.

***N*-(Quinolin-8-yl)butane-1-sulfonamide (12).**

Synthesized utilizing Sulfonamide Coupling method A using 1.5 equiv of sulfonyl chloride. Purified with a gradient of 0–15% EtOAc in hexanes. Isolated as dark oil. Yield = 0.090 g (49%). ¹H NMR (CDCl₃, 400 MHz) δ 8.89 (br, 1H), 8.80 (dd, *J*₁ = 4.0 Hz, *J*₂ = 1.6 Hz, 1H), 8.17 (dd, *J*₁ = 8.0 Hz, *J*₂ = 1.4 Hz, 1H), 7.84 (dd, *J*₁ = 7.2 Hz, *J*₂ = 1.6 Hz, 1H), 7.54–7.45 (m, 3H), 3.12 (m, 2H), 1.81 (m, 2H), 1.35 (sex, *J* = 7.2 Hz, 2H), 0.79 (t, *J* = 7.2 Hz, 3H). ESI-MS(+): *m/z* 265.12 [M+H]⁺.

***N*-(Quinolin-8-yl)cyclohexanesulfonamide (13).**

Synthesized utilizing Sulfonamide Coupling method A using 3 equiv of sulfonyl chloride. Purified with a gradient of 0–15% EtOAc in hexanes. Isolated as a clear oil. Yield = 0.034 g (17%). ¹H NMR (CDCl₃, 400 MHz) δ 8.85 (br, 1H), 8.81 (dd, *J*₁ = 4.4 Hz, *J*₂ = 1.6 Hz, 1H), 8.18 (dd, *J*₁ = 8.4 Hz, *J*₂ = 1.6 Hz, 1H), 7.88 (dd, *J*₁ = 7.2 Hz, *J*₂ = 1.6 Hz, 1H), 7.53–7.46 (m, 3H), 3.09 (tt, *J*₁ = 7.2 Hz, *J*₂ = 3.6 Hz, 1H), 2.18–1.14 (m, 10H). ESI-MS(+): *m/z* 291.17 [M+H]⁺, 313.13 [M+Na]⁺.

***N*-(Quinolin-8-yl)thiophene-2-sulfonamide (14).**

Synthesized utilizing Sulfonamide Coupling method B. Isolated as dark brown solid. Yield = 0.179 g (89%). ¹H NMR (400 MHz, CDCl₃): δ 9.30 (br, 1H), 8.76 (dd, *J*₁ = 4.4 Hz, *J*₂ = 1.6 Hz, 1H), 8.12 (dd, *J*₁ = 8.4 Hz, *J*₂ = 1.6 Hz, 1H), 7.91 (dd, *J*₁ = 6.4 Hz, *J*₂ = 2.4 Hz, 1H), 7.62 (dd, *J*₁ = 3.6 Hz, *J*₂ = 1.2 Hz, 1H), 7.51 (m, 2H), 7.44 (d, *J* = 4.4 Hz, 1H), 7.42 (d, *J* = 4.0 Hz, 1H), 6.92 (t, *J* = 3.6 Hz, 1H). ESI-MS(+): *m/z* 291.02 [M+H]⁺, 312.97 [M+Na]⁺.

1-Methyl-*N*-(quinolin-8-yl)-1*H*-imidazole-4-sulfonamide (15).

Synthesized utilizing Sulfonamide Coupling method A using 1.5 equiv of sulfonyl chloride. Product precipitated as H₂O was added to reaction mixture. The solid was isolated via filtration and not further purified. Isolated as pink solid. Yield = 0.089 g (48%). ¹H NMR (CDCl₃, 400 MHz) δ 9.41 (br, 1H), 8.79 (dd, *J*₁ = 4.0 Hz, *J*₂ = 1.6 Hz, 1H), 8.12 (dd, *J*₁ = 8.0 Hz, *J*₂ = 1.6 Hz, 1H), 7.89 (t, *J* = 4.4 Hz, 1H), 7.54 (d, *J* = 1.2 Hz, 1H), 7.46–7.41 (m, 3H), 7.36 (s, 1H), 7.25 (s, 1H), 3.65 (s, 3H). ESI-MS(+): *m/z* 289.22 [M+H]⁺, 311.16 [M+Na]⁺.

4-(1*H*-Pyrazol-1-yl)-*N*-(quinolin-8-yl)benzenesulfonamide (16).

Synthesized utilizing Sulfonamide Coupling method B. Isolated as a white solid. Yield = 0.330 g (99%). ¹H NMR (CDCl₃, 400 MHz) δ 9.26 (br, 1H), 8.76 (dd, *J*₁ = 4.0 Hz, *J*₂ = 1.6 Hz, 1H), 8.10 (dd, *J*₁ = 8.4 Hz, *J*₂ = 1.6 Hz, 1H), 7.98 (d, *J* = 9.2 Hz, 2H), 7.88 (d, *J* = 2.8

Hz, 1H), 7.86 (dd, $J_1 = 6.8$ Hz, $J_2 = 2.0$ Hz, 1H), 7.68 (d, $J = 2.0$ Hz, 1H), 7.68 (d, $J = 8.8$ Hz, 2H), 7.43 (m, 3H), 6.45 (dd, $J_1 = 2.8$ Hz, $J_2 = 2.0$ Hz, 1H). ESI-MS(+): m/z 351.08 [M+H]⁺, 373.06 [M+Na]⁺.

2-Methoxy-*N*-(quinolin-8-yl)benzenesulfonamide (17).

Synthesized utilizing Sulfonamide Coupling method A. Purified with a gradient of 0–25% EtOAc in hexanes. Isolated as white solid. Yield = 0.123 g (56%). ¹H NMR (CDCl₃, 400 MHz) δ 9.70 (br, 1H), 8.79 (dd, $J_1 = 4.0$ Hz, $J_2 = 1.6$ Hz, 1H), 8.07 (dd, $J_1 = 8.4$ Hz, $J_2 = 1.6$ Hz, 1H), 7.98 (dd, $J_1 = 8.4$ Hz, $J_2 = 1.6$ Hz, 1H), 7.81 (dd, $J_1 = 8.4$ Hz, $J_2 = 1.6$ Hz, 1H), 7.42–7.32 (m, 3H), 6.94 (t, $J = 8.4$ Hz, 1H), 6.78 (t, $J = 8.4$ Hz, 1H), 3.81 (s, 3H). ESI-MS(+): m/z 315.09 [M+H]⁺.

3-Methoxy-*N*-(quinolin-8-yl)benzenesulfonamide (18).

Synthesized utilizing Sulfonamide Coupling method A using 1.5 equiv of sulfonyl chloride. Purified with a gradient of 0–25% EtOAc in hexanes. Isolated as white solid. Yield = 0.20 g (92%). ¹H NMR (CDCl₃, 400 MHz) δ 9.25 (br, 1H), 8.67 (dd, $J_1 = 4.0$ Hz, $J_2 = 1.6$ Hz, 1H), 8.00 (dd, $J_1 = 8.4$ Hz, $J_2 = 1.6$ Hz, 1H), 7.84 (m, 1H), 7.48 (m, 1H), 7.39 (m, 3H), 7.33 (dd, $J_1 = 8.4$ Hz, $J_2 = 4.4$ Hz, 1H), 7.20 (t, $J_1 = 8.0$ Hz, 1H), 6.88 (m, 1H), 3.63 (s, 3H). ESI-MS(+): m/z 315.13 [M+H]⁺.

4-Methoxy-*N*-(quinolin-8-yl)benzenesulfonamide (19).

Synthesized utilizing Sulfonamide Coupling method B. Isolated as an off-white solid. Yield = 0.117 g (54%). ¹H NMR (400 MHz, CDCl₃): δ 9.20 (br, 1H), 8.76 (dd, $J_1 = 4.4$ Hz, $J_2 = 1.6$ Hz, 1H), 8.09 (dd, $J_1 = 8.0$ Hz, $J_2 = 1.6$ Hz, 1H), 7.85 (d, $J = 8.8$ Hz, 2H), 7.80 (dd, $J_1 = 6.0$ Hz, $J_2 = 2.4$ Hz, 1H), 7.43 (m, 3H), 6.81 (d, $J = 8.8$ Hz, 2H), 3.75 (s, 3H). ESI-MS(+): m/z 315.02 [M+H]⁺.

2-Cyano-*N*-(quinolin-8-yl)benzenesulfonamide (20).

Synthesized utilizing Sulfonamide Coupling method A. Purified with a gradient of 0–70% EtOAc in hexanes. Isolated as white solid. Yield = 0.070 g (33%). ¹H NMR (400 MHz, CDCl₃): δ 8.80 (dd, $J_1 = 4.0$ Hz, $J_2 = 1.6$ Hz, 1H), 8.18 (dd, $J_1 = 8.0$ Hz, $J_2 = 1.2$ Hz, 1H), 8.09 (dd, $J_1 = 8.4$ Hz, $J_2 = 1.6$ Hz, 1H), 7.73–7.39 (m, 7H). ESI-MS(+): m/z 310.11 [M+H]⁺.

3-Cyano-*N*-(quinolin-8-yl)benzenesulfonamide (21).

Synthesized utilizing Sulfonamide Coupling method A using 1.5 equiv of sulfonyl chloride. Purified with a gradient of 0–70% EtOAc in hexanes. Isolated as white solid. Yield = 0.070 g (32%). ¹H NMR (CDCl₃, 400 MHz) δ 9.25 (br, 1H), 8.77 (dd, $J_1 = 4.4$ Hz, $J_2 = 1.6$ Hz, 1H), 8.17–8.09 (m, 3H), 7.86 (dd, $J_1 = 7.2$ Hz, $J_2 = 1.2$ Hz, 1H), 7.70 (dd, $J_1 = 8.0$ Hz, $J_2 = 1.2$ Hz, 1H), 7.54–7.42 (m, 4H). ESI-MS(+): m/z 310.11 [M+H]⁺.

4-Cyano-*N*-(quinolin-8-yl)benzenesulfonamide (22).

Synthesized utilizing Sulfonamide Coupling method B. Isolated as an orange solid. Yield = 0.106 g (99%). ¹H NMR (CDCl₃, 400 MHz) δ 9.27 (br, 1H), 8.76 (dd, $J_1 = 4.4$ Hz, $J_2 = 1.6$ Hz, 1H), 8.12 (dd, $J_1 = 8.4$ Hz, $J_2 = 1.6$ Hz, 1H), 7.99 (d, $J = 8.0$ Hz, 2H), 7.85 (dd, $J_1 = 7.2$

Hz, $J_2 = 1.2$ Hz, 1H), 7.63 (d, $J = 8.0$ Hz, 2H), 7.53 (dd, $J_1 = 8.4$ Hz, $J_2 = 1.2$ Hz, 1H), 7.46 (m, 2H). ESI-MS(+): m/z 310.07 [M+H]⁺.

***N*-(Quinolin-8-yl)pyridine-2-sulfonamide (23).**

Synthesized utilizing Sulfonamide Coupling method A using 1.5 equiv of sulfonyl chloride. Purified with a gradient of 0–50% EtOAc in hexanes. Isolated as brown solid. Yield = 0.112 g (57%). ¹H NMR (CDCl₃, 400 MHz) δ 9.94 (br, 1H), 8.85 (m, 1H), 8.59 (m, 1H), 8.37 (dd, $J_1 = 8.4$ Hz, $J_2 = 2.0$ Hz, 1H), 8.09 (m, 2H), 7.76–7.48 (m, 5H). ESI-MS(+): m/z 286.12 [M+H]⁺.

***N*-(Quinolin-8-yl)pyridine-3-sulfonamide (24).**

Synthesized utilizing Sulfonamide Coupling method A using 1.1 equiv of sulfonyl chloride. Product precipitated as H₂O was added to reaction mixture. The solid was isolated via filtration and not further purified. Isolated as white solid. Yield = 0.198 g (99%). ¹H NMR (CDCl₃, 400 MHz) δ 9.33 (br, 1H), 9.07 (dd, $J_1 = 2.4$ Hz, $J_2 = 0.8$ Hz, 1H), 8.70 (dd, $J_1 = 4.4$ Hz, $J_2 = 1.6$ Hz, 1H), 8.60 (dd, $J_1 = 4.8$ Hz, $J_2 = 1.6$ Hz, 1H), 8.14 (m, 1H), 8.06 (dd, $J_1 = 8.0$ Hz, $J_2 = 1.6$ Hz, 1H), 7.85 (dd, $J_1 = 7.2$ Hz, $J_2 = 1.6$ Hz, 1H), 7.47–7.39 (m, 2H), 7.38 (dd, $J_1 = 8.4$ Hz, $J_2 = 4.4$ Hz, 1H), 7.25 (m, 1H). ESI-MS(+): m/z 286.10 [M+H]⁺, 307.99 [M+Na]⁺.

6-Morpholino-*N*-(quinolin-8-yl)pyridine-3-sulfonamide (25).

Synthesized utilizing Sulfonamide Coupling method B. Isolated as a white solid. Yield = 0.100 g (78%). ¹H NMR (CDCl₃, 400 MHz) δ 9.20 (br, 1H), 8.76 (dd, $J_1 = 4.4$ Hz, $J_2 = 1.6$ Hz, 1H), 8.65 (m, 1H), 8.10 (dd, $J_1 = 8.0$ Hz, $J_2 = 1.6$ Hz, 1H), 7.87 (dd, $J_1 = 9.2$ Hz, $J_2 = 2.8$ Hz, 1H), 7.82 (m, 1H), 7.45 (m, 3H), 6.45 (d, $J = 9.2$ Hz, 1H), 3.72 (m, 4H), 3.54 (m, 4H). ESI-MS(+): m/z 371.10 [M+H]⁺, 393.17 [M+Na]⁺.

4-(*tert*-Butyl)-*N*-(quinolin-8-yl)benzenesulfonamide (26).

Synthesized utilizing method Sulfonamide Coupling B. Isolated as a white solid. Yield = 0.216 g (91%). ¹H NMR (CDCl₃, 400 MHz) δ 9.23 (br, 1H), 8.75 (dd, $J_1 = 4.4$ Hz, $J_2 = 2.0$ Hz, 1H), 8.10 (dd, $J_1 = 8.4$ Hz, $J_2 = 1.6$ Hz, 1H), 7.83 (m, 3H), 7.43 (m, 3H), 7.37 (d, $J = 8.8$ Hz, 2H), 1.24 (s, 9H). ESI-MS(+): m/z 341.08 [M+H]⁺.

4-Fluoro-*N*-(quinolin-8-yl)benzenesulfonamide (27).

Synthesized utilizing Sulfonamide Coupling method B. Isolated as an amber solid. Yield = 0.150 g (72%). ¹H NMR (CDCl₃, 400 MHz) δ 8.77 (dd, $J_1 = 4.0$ Hz, $J_2 = 1.6$ Hz, 1H), 8.21 (dd, $J_1 = 8.4$ Hz, $J_2 = 1.6$ Hz, 1H), 7.88–7.92 (m, 2H), 7.83 (dd, $J_1 = 7.6$ Hz, $J_2 = 1.2$ Hz, 1H), 7.58 (dd, $J_1 = 8.0$ Hz, $J_2 = 1.2$ Hz, 1H), 7.46–7.50 (m, 2H), 7.09 (t, $J = 8.4$ Hz, 2H). ESI-MS(+): m/z 303.05 [M+H]⁺, 324.99 [M+Na]⁺.

3,4-Difluoro-*N*-(quinolin-8-yl)benzenesulfonamide (28).

Synthesized utilizing Sulfonamide Coupling method A using 1.1 equiv of sulfonyl chloride. Purified with a gradient of 0–20% EtOAc in hexanes. Isolated as a brown solid. Yield = 0.10 g (46%). ¹H NMR (CDCl₃, 400 MHz) δ 8.75 (dd, $J_1 = 4.0$ Hz, $J_2 = 1.6$ Hz, 1H), 8.11 (dd, J_1

= 8.0 Hz, $J_2 = 1.2$ Hz, 1H), 7.84 (dd, $J_1 = 7.2$ Hz, $J_2 = 1.2$ Hz, 1H), 7.76–7.66 (m, 2H), 7.51–7.40 (m, 3H), 7.13 (m, 1H). ESI-MS(+): m/z 321.11 [M+H]⁺.

***N*-(Quinolin-8-yl)benzo[d][1,3]dioxole-5-sulfonamide (29).**

Synthesized utilizing Sulfonamide Coupling method B. Isolated as a dark brown solid. Yield = 0.08 g (70%). ¹H NMR (CDCl₃, 400 MHz) δ 9.20 (br, 1H), 8.77 (dd, $J_1 = 4.4$ Hz, $J_2 = 1.6$ Hz, 1H), 8.11 (dd, $J_1 = 8.4$ Hz, $J_2 = 1.6$ Hz, 1H), 7.80 (dd, $J_1 = 6.4$ Hz, $J_2 = 2.4$ Hz, 1H), 7.50 (dd, $J_1 = 8.0$ Hz, $J_2 = 2.0$ Hz, 1H), 7.45 (m, 2H), 7.43 (t, $J = 4.0$ Hz, 1H), 7.31 (d, $J = 2.0$ Hz, 1H), 6.73 (d, $J = 8.4$ Hz, 1H), 5.96 (s, 2H). ESI-MS(+): m/z 329.09 [M+H]⁺.

2-Oxo-*N*-(quinolin-8-yl)indoline-5-sulfonamide (30).

Synthesized utilizing Sulfonamide Coupling method B. Isolated as an orange solid. Yield = 0.09 g (91%). ¹H NMR (CDCl₃, 400 MHz) δ 10.72 (br, 1H), 9.80 (br, 1H), 8.86 (dd, $J_1 = 4.0$ Hz, $J_2 = 1.6$ Hz, 1H), 8.34 (dd, $J_1 = 8.0$ Hz, $J_2 = 1.6$ Hz, 1H), 7.76 (m, 2H), 7.60 (m, 3H), 7.50 (t, $J = 8.0$ Hz, 1H), 6.82 (d, $J = 8.8$ Hz, 1H), 3.47 (s, 2H). ESI-MS(+): m/z 340.09 [M+H]⁺.

***N*-(Quinolin-8-yl)naphthalene-2-sulfonamide (31).**

Synthesized utilizing Sulfonamide Coupling method B. Isolated as a white solid. Yield = 0.20 g (87%). ¹H NMR (CDCl₃, 400 MHz) δ 9.35 (br, 1H), 8.76 (dd, $J_1 = 4.4$ Hz, $J_2 = 1.6$ Hz, 1H), 8.51 (d, $J = 2.0$ Hz, 1H), 8.06 (dd, $J_1 = 8.0$ Hz, $J_2 = 1.6$ Hz, 1H), 7.88 (m, 3H), 7.78 (m, 2H), 7.55 (m, 2H), 7.41 (m, 3H). ESI-MS(+): m/z 335.04 [M+H]⁺.

***N*-(Quinolin-8-yl)benzo[d]thiazole-6-sulfonamide (32).**

Synthesized utilizing Sulfonamide Coupling method A using 1.1 equiv of sulfonyl chloride. Purified with a gradient of 0–40% EtOAc in hexanes. Isolated as an off-white solid. Yield = 0.11 g (45%). ¹H NMR (400 MHz, CDCl₃): δ 9.33 (br, 1H), 9.07 (s, 1H), 8.72 (d, $J = 4.4$ Hz, 1H), 8.58 (s, 1H), 8.05 (m, 3H), 7.88 (m, 1H), 7.43 (m, 2H), 7.38 (m, 1H). ESI-MS(+): m/z 342.03 [M+H]⁺, 363.99 [M+Na]⁺.

2-(Methylthio)-*N*-(quinolin-8-yl)benzo[d]thiazole-6-sulfonamide (33).

Synthesized utilizing Sulfonamide Coupling method B. Isolated as a light brown solid. Yield = 0.20 g (81%). ¹H NMR (CDCl₃, 400 MHz) δ 9.28 (br, 1H), 8.74 (dd, $J_1 = 4.4$ Hz, $J_2 = 1.6$ Hz, 1H), 8.41 (dd, $J_1 = 1.6$ Hz, $J_2 = 0.4$ Hz, 1H), 8.08 (dd, $J_1 = 8.4$ Hz, $J_2 = 1.6$ Hz, 1H), 7.90 (dd, $J_1 = 8.8$ Hz, $J_2 = 1.6$ Hz, 1H), 7.90 (dd, $J_1 = 8.4$ Hz, $J_2 = 1.6$ Hz, 1H), 7.85 (dd, $J_1 = 6.4$ Hz, $J_2 = 2.8$ Hz, 1H), 7.75 (dd, $J_1 = 8.4$ Hz, $J_2 = 0.4$ Hz, 1H), 7.42 (m, 3H). ESI-MS(+): m/z 388.05 [M+H]⁺.

1-Phenyl-*N*-(quinolin-8-yl)methanesulfonamide (34).

Synthesized utilizing Sulfonamide Coupling method B. Isolated as a yellow solid. Yield = 0.20 g (97%). ¹H NMR (CDCl₃, 400 MHz) δ 8.87 (br, 1H), 8.71 (dd, $J_1 = 4.4$ Hz, $J_2 = 1.6$ Hz, 1H), 8.18 (dd, $J_1 = 8.4$ Hz, $J_2 = 1.6$ Hz, 1H), 7.80 (dd, $J_1 = 7.6$ Hz, $J_2 = 1.6$ Hz, 1H), 7.54 (dd, $J_1 = 8.8$ Hz, $J_2 = 1.2$ Hz, 1H), 7.48 (m, 2H), 7.25 (m, 1H), 7.15 (t, $J = 8.0$ Hz, 2H), 7.08 (d, $J = 7.2$ Hz, 2H). ESI-MS(+): m/z 299.06 [M+H]⁺, 321.08 [M+Na]⁺.

2-Phenyl-*N*-(quinolin-8-yl)ethane-1-sulfonamide (35).

Synthesized utilizing Sulfonamide Coupling method A using 1.5 equiv of sulfonyl chloride. Purified with a gradient of 0–20% EtOAc in hexanes. Isolated as a tan solid. Yield = 0.143 g (66%). ¹H NMR (CDCl₃, 400 MHz) δ 8.96 (br, 1H), 8.81 (d, *J* = 4.0 Hz, 1H), 8.19 (d, *J* = 8.4 Hz, 1H), 7.90 (d, *J* = 8.4 Hz, 1H), 7.58–7.47 (m, 3H), 7.18–7.11 (m, 3H), 6.97 (d, *J* = 8.4 Hz, 3H), 3.40 (t, *J* = 8.0 Hz, 2H), 3.40 (t, *J* = 8.0 Hz, 2H), 3.16 (t, *J* = 8.0 Hz, 2H). ESI-MS(+): *m/z* 313.18 [M+H]⁺.

3-Phenyl-*N*-(quinolin-8-yl)propane-1-sulfonamide (36).

Synthesized utilizing Sulfonamide Coupling method A using 1.1 equiv of sulfonyl chloride. Purified with a gradient of 0–30% EtOAc in hexanes. Isolated as a tan solid. Yield = 0.185 g (82%). ¹H NMR (CDCl₃, 400 MHz) δ 9.23 (br, 1H), 8.69 (dd, *J*₁ = 4.4 Hz, *J*₂ = 1.6 Hz, 1H), 8.01 (dd, *J*₁ = 8.4 Hz, *J*₂ = 1.6 Hz, 1H), 7.83 (m, 3H), 7.39 (d, *J* = 4.8 Hz, 2H), 7.34 (dd, *J*₁ = 8.0 Hz, *J*₂ = 4.0 Hz, 1H), 7.12 (d, *J* = 8.4 Hz, 2H), 2.48 (t, *J* = 7.6 Hz, 2H), 1.53 (sex, *J* = 7.6 Hz, 2H), 0.81 (t, *J* = 7.2 Hz, 3H). ESI-MS(+): *m/z* 327.09 [M+H]⁺, 349.03 [M+Na]⁺.

5-Bromo-8-nitroquinoline.

A solution of 5-bromoquinoline (10 g, 48.1 mmol) in concentrated H₂SO₄ (40 mL) was cooled to 0 °C under a nitrogen atmosphere. To this was added potassium nitrate (7.77 g, 77 mmol) slowly and portion-wise. The resulting reaction mixture was then allowed to warm up to room temperature slowly and then stirred for an additional 15 h at room temperature. The resulting mixture was then poured onto ice, which caused the formation of a precipitate. The precipitate was then filtered and rinsed with excess amount of H₂O. The resulting product was not further purified and was isolated as a light yellow solid. Yield = 10.63 g (87%). ¹H NMR (CDCl₃, 400 MHz) δ 9.08 (dd, *J*₁ = 4.0 Hz, *J*₂ = 1.6 Hz, 1H), 8.62 (dd, *J*₁ = 8.4 Hz, *J*₂ = 1.6 Hz, 1H), 7.90 (d, *J*₁ = 0.8 Hz, 2H), 7.67 (dd, *J*₁ = 8.4 Hz, *J*₂ = 4.0 Hz, 1H). ESI-MS(+): *m/z* 253.21, 255.17 [M+H]⁺.

Protocol for Suzuki Coupling Method A —To a solution of 5-bromo-8-nitroquinoline (0.3 g, 1.18 mmol) in H₂O (10 mL) was added a boronic acid (1.78 mmol), diisopropylamine (0.498 mL, 3.56 mmol), and palladium acetate (0.018 g, 0.08 mmol) and the solution was heated to reflux for 16 h. To the reaction mixture was added H₂O (50 mL) and the solution was extracted with EtOAc (3×50mL). The reaction mixture was filtered through celite, concentrated, and then the product was purified via silica gel chromatography utilizing a gradient of EtOAc in hexanes.

Protocol for Suzuki Coupling Method B —To a solution of 5-bromo-8-nitroquinoline (0.3 g, 1.18 mmol) in 1,4-dioxane (10 mL) was added a boronic acid (1.78 mmol), potassium acetate (0.233 g, 2.37 mmol), and Pd(PPh₃)₄ (0.068 g, 0.06 mmol) and the solution was degassed for 5–10 mins. The reaction mixture was then heated to reflux for 16 h under nitrogen atmosphere. The reaction mixture was filtered through celite, concentrated, and then the product was purified via silica gel chromatography utilizing a gradient of EtOAc in hexanes.

Protocol for Suzuki Coupling Method C —To a solution of 5-bromo-8-nitroquinoline (0.3 g, 1.18 mmol) in H₂O (5 mL) and 1,4-dioxane (5 mL) was added a boronic acid (1.78 mmol), potassium carbonate (0.328 g, 2.37 mmol), S-Phos (0.05 g, 0.12 mmol), and Pd(dppf)Cl₂·CH₂Cl₂ (0.097 g, 0.12 mmol), and the solution was degassed for 5–10 mins. The reaction mixture was then heated to reflux for 16 h under nitrogen atmosphere. The reaction mixture was filtered through celite, concentrated, and then the product was purified via silica gel chromatography utilizing a gradient of EtOAc in hexanes or MeOH in CH₂Cl₂.

Protocol for Buchwald Coupling —To a solution of 5-bromo-8-nitroquinoline (0.3 g, 1.18 mmol) in DMF (10 mL) was added an amine (3.56 mmol), potassium carbonate (0.49 g, 3.6 mmol), X-Phos (0.11 g, 0.24 mmol), Pd₂(dba)₃ (0.22 g, 0.24 mmol), and the solution was degassed for 5–10 mins. The reaction mixture was then irradiated in a microwave reactor at 140 °C for 30 min. The resulting mixture was filtered through celite, concentrated, and then the product was purified via silica gel chromatography utilizing a gradient of EtOAc in hexanes.

Protocol for Sonogashira Coupling —To a solution of 5-bromo-8-nitroquinoline (0.3 g, 1.18 mmol) in 1,4-dioxane (10 mL) and Et₃N (10 mL) was added an alkyne (1.78 mmol), X-Phos (0.057 g, 0.12 mmol), Pd(dppf)Cl₂·CH₂Cl₂ (0.097 g, 0.12 mmol), and CuI (0.023 g, 0.12 mmol) and the solution was degassed for 5–10 mins. The reaction mixture was then heated to reflux for 16 h under nitrogen atmosphere. The reaction mixture was filtered through celite, concentrated, then the product was purified via silica gel chromatography utilizing a gradient of EtOAc in hexanes.

8-Nitro-5-phenylquinoline.

Synthesized utilizing Suzuki coupling Method A. The product was purified with a gradient of 0–30% EtOAc in hexanes. The desired product was isolated as a light tan solid. Yield = 0.297 g (75%). ¹H NMR (CDCl₃, 400 MHz) δ 9.03 (d, *J* = 4.0 Hz, 1H), 8.30 (d, *J* = 4.0 Hz, 1H), 8.06 (d, *J* = 4.0 Hz, 1H), 7.56–7.43 (m, 7H). ESI-MS(+): *m/z* 251.34 [M+H]⁺.

8-Nitro-5-(pyridin-4-yl)quinoline.

Synthesized utilizing Suzuki coupling Method C. The product was purified with a gradient of 0–15% MeOH in CH₂Cl₂. Yield = 0.132 g (44%). ¹H NMR (CDCl₃, 400 MHz) δ 9.10 (dd, *J*₁ = 4 Hz, *J*₂ = 1.6 Hz, 1H), 8.81–8.80 (m, 2H), 8.23 (dd, *J*₁ = 8.8 Hz, *J*₂ = 1.6 Hz, 1H), 8.09 (d, *J* = 8.0 Hz, 1H), 7.59 (d, *J* = 8.0 Hz, 1H), 7.56 (dd, *J*₁ = 8.8 Hz, *J*₂ = 4.4 Hz, 1H), 7.40–7.39 (m, 2H). ESI-MS(+): *m/z* 252.25 [M+H]⁺.

8-Nitro-5-(pyrimidin-5-yl)quinoline.

Synthesized utilizing Suzuki coupling Method C. The product was purified with a gradient of 0–15% MeOH in CH₂Cl₂. Yield = 0.138 g (46%). ¹H NMR (CDCl₃, 400 MHz) δ 9.39 (s, 1H), 9.14 (d, *J* = 4.0 Hz, 1H), 8.90 (s, 2H), 8.17 (d, *J* = 8.8 Hz, 1H), 8.13 (d, *J* = 8.0 Hz, 1H), 7.63–7.60 (m, 2H). ESI-MS(+): *m/z* 253.43 [M+H]⁺.

5-(4-Chlorophenyl)-8-nitroquinoline.

Synthesized utilizing Suzuki coupling Method B. The product was purified via silica gel chromatography eluting a gradient of 0–30% EtOAc in hexanes. Yield = 0.182 g (54%). ¹H NMR (CDCl₃, 400 MHz) δ 9.03 (d, *J* = 4.0 Hz, 1H), 8.30 (d, *J* = 4.0 Hz, 1H), 8.06 (d, *J* = 4.0 Hz, 1H), 7.56–7.43 (m, 7H). ESI-MS(+): *m/z* 285.43 [M+H]⁺.

5-(3,4-Difluorophenyl)-8-nitroquinoline.

Synthesized utilizing Suzuki coupling Method A. The product was purified via silica gel chromatography eluting 0–40% EtOAc in hexanes. Yield = 0.311 g (92%). ¹H NMR (CDCl₃, 400 MHz) δ 9.09 (d, *J* = 4.0 Hz, 1H), 8.25 (d, *J* = 8.8 Hz, 1H), 8.07 (d, *J* = 8.0 Hz, 1H), 7.56–7.53 (m, 2H), 7.39–7.28 (m, 2H), 7.20–7.17 (m, 1H). ESI-MS(+): *m/z* 287.32 [M+H]⁺.

5-(Furan-2-yl)-8-nitroquinoline.

Synthesized utilizing Suzuki coupling Method B. The product was purified via silica gel chromatography eluting a gradient of 0–30% EtOAc in hexanes. Yield = 0.181 g (64%). ¹H NMR (CDCl₃, 400 MHz) δ 9.04 (d, *J* = 4.0 Hz, 1H), 8.88 (d, *J* = 8.0 Hz, 1H), 8.02 (d, *J* = 8.0 Hz, 1H), 7.80 (d, *J* = 8.0 Hz, 1H), 7.68 (m, 1H), 7.57 (dd, *J*₁ = 8.0 Hz, *J*₂ = 4.0 Hz, 1H), 6.84 (d, *J* = 2.4 Hz, 1H), 6.63 (m, 1H). ESI-MS(+): *m/z* 241.31 [M+H]⁺.

8-Nitro-5-(thiophen-2-yl)quinoline.

Synthesized utilizing Suzuki coupling Method B. Product was purified via silica gel chromatography eluting a gradient of 0–40% EtOAc in hexanes. Yield = 0.300 g (99%). ¹H NMR (CDCl₃, 400 MHz) δ 9.08 (m, 1H), 8.65 (d, *J* = 8.0 Hz, 1H), 8.04 (d, *J* = 8.0 Hz, 1H), 7.69 (d, *J* = 8.0 Hz, 1H), 7.55 (m, 2H), 7.27–7.24 (m, 2H). ESI-MS(+): *m/z* 257.27 [M+H]⁺.

5-(Benzo[*d*][1,3]dioxol-5-yl)-8-nitroquinoline.

Synthesized utilizing Suzuki coupling Method A. Product was purified via silica gel chromatography eluting 0–40% EtOAc in hexanes. Yield = 0.167 g (48%). ¹H NMR (CDCl₃, 400 MHz) δ 9.03 (d, *J* = 4.0 Hz, 1H), 8.34 (d, *J* = 8.8 Hz, 1H), 8.03 (d, *J* = 8.0 Hz, 1H), 7.52–7.47 (m, 2H), 6.96 (d, *J* = 8.0 Hz, 1H), 6.88–6.87 (m, 2H), 6.06 (s, 2H). ESI-MS(+): *m/z* 295.36 [M+H]⁺.

8-Nitro-5-(piperidin-1-yl)quinoline.

Synthesized utilizing Buchwald coupling Method. Product was purified with a gradient of 0–25% EtOAc in hexanes. Yield = 0.182 g (60%). ¹H NMR (CDCl₃, 400 MHz) δ 9.04 (dd, *J*₁ = 4.0 Hz, *J*₂ = 1.6 Hz, 1H), 8.47 (dd, *J*₁ = 8.4 Hz, *J*₂ = 1.6 Hz, 1H), 8.11 (d, *J* = 8.4 Hz, 1H), 7.49 (dd, *J*₁ = 8.4 Hz, *J*₂ = 4.0 Hz, 1H), 7.00 (d, *J* = 8.4 Hz, 1H), 3.14 (t, *J* = 5.6 Hz, 4H), 1.88 (pent, *J* = 5.6 Hz, 4H), 1.72 (m, 2H). ESI-MS(+): *m/z* 258.34 [M+H]⁺.

4-(8-Nitroquinolin-5-yl)morpholine.

Synthesized utilizing Buchwald coupling Method. Product was purified with a gradient of 0–25% EtOAc in hexanes. Yield = 0.202 g (68%). ¹H NMR (CDCl₃, 400 MHz) δ 9.00 (dd, *J*₁ = 4.0 Hz, *J*₂ = 1.6 Hz, 1H), 8.49 (dd, *J*₁ = 8.4 Hz, *J*₂ = 1.6 Hz, 1H), 8.05 (d, *J* = 8.4 Hz,

1H), 7.50 (dd, $J_1 = 8.4$ Hz, $J_2 = 4.0$ Hz, 1H), 7.04 (d, $J = 8.4$ Hz, 1H), 3.97 (t, $J = 4.4$ Hz, 4H), 3.16 (t, $J = 4.4$ Hz, 4H). ESI-MS(+): m/z 260.11 [M+H]⁺.

***N*-(5-Phenylquinolin-8-yl)methanesulfonamide (37).**

Synthesized utilizing Sulfonamide Coupling Method A. Product was purified with a gradient of 0–25% EtOAc in hexanes. Isolated as an off-white solid. Yield = 0.033 g (24%). ¹H NMR (CDCl₃, 400 MHz) δ 9.03 (br, 1H), 8.84 (d, $J = 3.6$ Hz, 1H), 8.31 (d, $J = 8.4$ Hz, 1H), 7.92 (d, $J = 8.4$ Hz, 1H), 7.51–7.43 (m, 7H), 3.08 (s, 3H). ESI-MS(+): m/z 299.10 [M+H]⁺.

***N*-(5-(Pyridin-4-yl)quinolin-8-yl)methanesulfonamide (38).**

Synthesized utilizing Sulfonamide Coupling Method A. Product was purified with a gradient of 0–10% MeOH in CH₂Cl₂. Isolated as an off-white solid. Yield = 0.054 g (35%). ¹H NMR (CDCl₃, 400 MHz) δ 9.09 (br, 1H), 8.86 (d, $J = 4.0$ Hz, 1H), 8.74 (d, $J = 5.2$ Hz, 2H), 8.25 (d, $J = 8.4$ Hz, 1H), 7.92 (d, $J = 8.4$ Hz, 1H), 7.51–7.47 (m, 2H), 7.39 (m, 2H), 3.09 (s, 3H). ESI-MS(+): m/z 300.14 [M+H]⁺.

***N*-(5-(Pyrimidin-5-yl)quinolin-8-yl)methanesulfonamide (39).**

Synthesized utilizing Sulfonamide Coupling Method A. Product was purified with a gradient of 0–10% MeOH in CH₂Cl₂. Isolated as an off-white solid. Yield = 0.048 g (32%). ¹H NMR (CDCl₃, 400 MHz) δ 9.29 (s, 1H), 9.12 (br, 1H), 8.88 (d, $J = 4.0$ Hz, 1H), 8.85 (s, 2H), 8.14 (d, $J = 8.4$ Hz, 1H), 7.94 (d, $J = 8.4$ Hz, 1H), 7.55 (dd, $J_1 = 8.4$ Hz, $J_2 = 4.0$ Hz, 1H), 7.51 (d, $J = 8.4$ Hz, 1H), 3.09 (s, 3H). ESI-MS(+): m/z 301.10 [M+H]⁺.

***N*-(5-(4-Chlorophenyl)quinolin-8-yl)methanesulfonamide (40).**

Synthesized utilizing Sulfonamide Coupling Method A. Product was purified with a gradient of 0–40% EtOAc in hexanes. Isolated as an off-white solid. Yield = 0.042 g (24%). ¹H NMR (CDCl₃, 400 MHz) δ 9.03 (br, 1H), 8.85 (dd, $J_1 = 4.0$ Hz, $J_2 = 1.6$ Hz, 1H), 8.24 (dd, $J_1 = 4.0$ Hz, $J_2 = 1.6$ Hz, 1H), 7.91 (d, $J = 8.0$ Hz, 1H), 7.49–7.38 (m, 6H), 3.07 (s, 3H). ESI-MS(+): m/z 333.23 [M+H]⁺.

***N*-(5-(3,4-Difluorophenyl)quinolin-8-yl)methanesulfonamide (41).**

Synthesized utilizing Sulfonamide Coupling Method A. Product was purified with a gradient of 0–35% EtOAc in hexanes. Isolated as a tan solid. Yield = 0.068 g (39%). ¹H NMR (CDCl₃, 400 MHz) δ 9.04 (br, 1H), 8.85 (dd, $J_1 = 4.0$ Hz, $J_2 = 1.6$ Hz, 1H), 8.23 (dd, $J_1 = 4.0$ Hz, $J_2 = 1.6$ Hz, 1H), 7.89 (d, $J = 8.0$ Hz, 1H), 7.51 (dd, $J_1 = 8.0$ Hz, $J_2 = 4.0$ Hz, 1H), 7.46 (d, $J = 8.0$ Hz, 1H), 7.33–7.14 (m, 3H), 3.08 (s, 3H). ESI-MS(+): m/z 335.41 [M+H]⁺.

***N*-(5-(Furan-2-yl)quinolin-8-yl)methanesulfonamide (42).**

Synthesized utilizing Sulfonamide Coupling Method A. Product was purified with a gradient of 0–25% EtOAc in hexanes. Isolated as a red-brown oil. Yield = 0.091 g (42%). ¹H NMR (CDCl₃, 400 MHz) δ 9.03 (br, 1H), 8.81–8.77 (m, 2H), 7.86 (d, $J = 8.0$ Hz, 1H), 7.73 (d, $J = 8.0$ Hz, 1H), 7.61 (d, $J = 1.6$ Hz, 1H), 7.53 (dd, $J_1 = 8.0$ Hz, $J_2 = 4.0$ Hz, 1H), 6.66 (d, $J = 3.2$ Hz, 1H), 6.58 (dd, $J_1 = 3.2$ Hz, $J_2 = 1.6$ Hz, 1H), 3.04 (s, 3H). ESI-MS(+): m/z 289.13 [M+H]⁺.

N-(5-(Thiophen-2-yl)quinolin-8-yl)methanesulfonamide (43).

Synthesized utilizing Sulfonamide Coupling Method A. Product was purified with a gradient of 0–55% EtOAc in hexanes. Isolated as faint yellow crystals. Yield = 0.128 g (68%). ¹H NMR (CDCl₃, 400 MHz) δ 9.05 (br, 1H), 8.84 (dd, *J*₁ = 4.0 Hz, *J*₂ = 1.6 Hz, 1H), 8.58 (dd, *J*₁ = 8.0 Hz, *J*₂ = 1.6 Hz, 1H), 7.88 (d, *J* = 8.0 Hz, 1H), 7.62 (d, *J* = 8.0 Hz, 1H), 7.52 (dd, *J*₁ = 8.0 Hz, *J*₂ = 4.0 Hz, 1H), 7.45 (dd, *J*₁ = 4.0 Hz, *J*₂ = 1.6 Hz, 1H), 7.20–7.18 (m, 2H), 3.07 (s, 3H). ESI-MS(+): *m/z* 305.33 [M+H]⁺.

N-(5-(Benzo[d][1,3]dioxol-5-yl)quinolin-8-yl)methanesulfonamide (44).

Synthesized utilizing Sulfonamide Coupling Method A. Product was purified with a gradient of 0–50% EtOAc in hexanes. Isolated as a faint yellow solid. Yield = 0.086 g (46%). ¹H NMR (CDCl₃, 400 MHz) δ 9.00 (br, 1H), 8.83 (dd, *J*₁ = 4.0 Hz, *J*₂ = 1.6 Hz, 1H), 8.33 (dd, *J*₁ = 8.0 Hz, *J*₂ = 1.6 Hz, 1H), 7.88 (d, *J* = 8.0 Hz, 1H), 7.47–7.44 (m, 2H), 6.95–6.87 (m, 3H), 6.05 (s, 2H), 3.06 (s, 3H). ESI-MS(+): *m/z* 343.17 [M+H]⁺.

N-(5-(Piperidin-1-yl)quinolin-8-yl)methanesulfonamide (45).

Synthesized utilizing Sulfonamide Coupling Method A. Product was purified with a gradient of 0–75% EtOAc in hexanes. Isolated as a yellow solid. Yield = 0.091 g (48%). ¹H NMR (CDCl₃, 400 MHz) δ 8.80 (dd, *J*₁ = 4.0 Hz, *J*₂ = 1.6 Hz, 1H), 8.67 (br, 1H), 8.54 (dd, *J*₁ = 8.0 Hz, *J*₂ = 1.6 Hz, 1H), 7.77 (d, *J* = 8.0 Hz, 1H), 7.48 (dd, *J*₁ = 8.0 Hz, *J*₂ = 4.0 Hz, 1H), 7.08 (d, *J* = 8.0 Hz, 1H), 3.03–2.95 (m, 4H), 2.94 (s, 3H), 1.85 (pent, 4H), 1.66 (br, 2H). ESI-MS(+): *m/z* 306.11 [M+H]⁺.

N-(5-Morpholinoquinolin-8-yl)methanesulfonamide (46).

Synthesized utilizing Sulfonamide Coupling Method A. Product was purified with a gradient of 0–75% EtOAc in hexanes. Isolated as a yellow solid. Yield = 0.101 g (51%). ¹H NMR (CDCl₃, 400 MHz) δ 8.82 (dd, *J*₁ = 4.0 Hz, *J*₂ = 2.0 Hz, 1H), 8.72 (br, 1H), 8.56 (dd, *J*₁ = 8.4 Hz, *J*₂ = 2.0 Hz, 1H), 7.79 (d, *J* = 8.4 Hz, 1H), 7.50 (dd, *J*₁ = 8.4 Hz, *J*₂ = 4.0 Hz, 1H), 7.14 (d, *J* = 8.4 Hz, 1H), 3.97 (t, *J* = 4.4 Hz, 4H), 3.07 (t, *J* = 4.4 Hz, 4H), 2.97 (s, 3H). ESI-MS(+): *m/z* 308.54 [M+H]⁺.

5-(3-Chlorophenyl)-8-nitroquinoline.

Synthesized utilizing Suzuki coupling Method B. Product was purified with a gradient of 0–35% EtOAc in hexanes. Isolated as a tan solid. Yield = 0.222 g (65%). ¹H NMR (CDCl₃, 400 MHz) δ 9.01 (m, 1H), 8.24 (m, 1H), 8.03 (d, *J* = 8.4 Hz, 1H), 7.54–7.19 (m, 6H). ESI-MS(+): *m/z* 285.24 [M+H]⁺.

5-(4-Fluorophenyl)-8-nitroquinoline.

Synthesized utilizing Suzuki coupling Method C. Product was purified with a gradient of 0–35% EtOAc in hexanes. Isolated as a brown solid. Yield = 0.167 g (53%). ¹H NMR (CDCl₃, 400 MHz) δ 9.02 (dd, *J*₁ = 4.0 Hz, *J*₂ = 1.6 Hz, 1H), 8.25 (dd, *J*₁ = 8.4 Hz, *J*₂ = 1.6 Hz, 1H), 8.04 (d, *J* = 8.4 Hz, 1H), 7.55 (d, *J* = 8.4 Hz, 1H), 8.25 (dd, *J*₁ = 8.4 Hz, *J*₂ = 4.0 Hz, 1H), 7.43–7.40 (m, 2H), 7.24–7.20 (m, 2H). ESI-MS(+): *m/z* 269.19 [M+H]⁺.

5-(4-Methoxyphenyl)-8-nitroquinoline.

Synthesized utilizing Suzuki coupling Method C. Product was purified with a gradient of 0–50% EtOAc in hexanes. Isolated as a tan solid. Yield = 0.110 g (33%). ¹H NMR (CDCl₃, 400 MHz) δ 9.05 (dd, *J*₁ = 4.0 Hz, *J*₂ = 1.6 Hz, 1H), 8.33 (dd, *J*₁ = 8.8 Hz, *J*₂ = 2.0 Hz, 1H), 8.06 (d, *J* = 8.0 Hz, 1H), 7.57 (d, *J* = 8.0 Hz, 1H), 7.51 (dd, *J*₁ = 8.8 Hz, *J*₂ = 4.0 Hz, 1H), 7.46 (t, *J* = 8.0 Hz, 1H), 7.06–6.97 (m, 3H), 3.86 (s, 3H). ESI-MS(+): *m/z* 281.31 [M+H]⁺.

5-(3-Methoxyphenyl)-8-nitroquinoline.

Synthesized utilizing Suzuki coupling Method C. Product was purified with a gradient of 0–50% EtOAc in hexanes. Isolated as a tan solid. Yield = 0.249 g (75%). ¹H NMR (CDCl₃, 400 MHz) δ 9.03 (dd, *J*₁ = 4.0 Hz, *J*₂ = 1.6 Hz, 1H), 8.33 (dd, *J*₁ = 8.8 Hz, *J*₂ = 1.6 Hz, 1H), 8.05 (d, *J* = 8.0 Hz, 1H), 7.53 (d, *J* = 8.0 Hz, 1H), 7.49 (dd, *J*₁ = 8.8 Hz, *J*₂ = 4.0 Hz, 1H), 7.37 (d, *J* = 8.4 Hz, 1H), 7.07 (d, *J* = 8.4 Hz, 1H), 3.89 (s, 3H). ESI-MS(+): *m/z* 281.19 [M+H]⁺.

5-(3-Chloro-4-methoxyphenyl)-8-nitroquinoline.

Synthesized utilizing Suzuki coupling Method B. Product was purified with a gradient of 0–60% EtOAc in hexanes. Isolated as a tan solid. Yield = 0.30 g (68%). ¹H NMR (CDCl₃, 400 MHz) δ 9.06 (dd, *J*₁ = 4.0 Hz, *J*₂ = 1.6 Hz, 1H), 8.30 (dd, *J*₁ = 8.4 Hz, *J*₂ = 2.0 Hz, 1H), 8.06 (d, *J* = 8.0 Hz, 1H), 7.54–7.46 (m, 3H), 7.33 (dd, *J*₁ = 8.4 Hz, *J*₂ = 2.0 Hz, 1H), 7.11 (d, *J* = 8.4 Hz, 1H), 4.00 (s, 3H). ESI-MS(+): *m/z* 315.15 [M+H]⁺.

5-(3,4-Dichlorophenyl)-8-nitroquinoline.

Synthesized utilizing Suzuki coupling Method B. Product was purified with a gradient of 0–50% EtOAc in hexanes. Isolated as a tan solid. Yield = 0.30 g (75%). ¹H NMR (CDCl₃, 400 MHz) δ 9.05 (dd, *J*₁ = 4.0 Hz, *J*₂ = 1.6 Hz, 1H), 8.30–8.05 (m, 2H), 7.54–7.46 (m, 3H), 7.32 (dd, *J*₁ = 8.4 Hz, *J*₂ = 2.0 Hz, 1H), 7.11 (d, *J* = 8.4 Hz, 1H), 4.00 (s, 3H). ESI-MS(+): *m/z* 319.23 [M+H]⁺.

5-(3,5-Dimethoxyphenyl)-8-nitroquinoline.

Synthesized utilizing Suzuki coupling Method C. Product was purified with a gradient of 0–35% EtOAc in hexanes. Isolated as a brown solid. Yield = 0.19 g (53%). ¹H NMR (CDCl₃, 400 MHz) δ 9.07 (dd, *J*₁ = 4.0 Hz, *J*₂ = 1.6 Hz, 1H), 8.36 (dd, *J*₁ = 8.8 Hz, *J*₂ = 1.6 Hz, 1H), 8.06 (d, *J* = 8.0 Hz, 1H), 7.58 (d, *J* = 8.0 Hz, 1H), 7.51 (dd, *J*₁ = 8.8 Hz, *J*₂ = 4.0 Hz, 1H), 6.60–6.55 (m, 3H), 3.84 (s, 6H). ESI-MS(+): *m/z* 311.26 [M+H]⁺.

8-Nitro-5-(phenylethynyl)quinoline.

Synthesized utilizing Sonogashira coupling method. Product was purified with a gradient of 0–35% EtOAc in hexanes. Isolated as a brown solid. Yield = 0.206 g (63%). ¹H NMR (CDCl₃, 400 MHz) δ 9.11 (m, 1H), 8.79 (dd, *J*₁ = 8.8 Hz, *J*₂ = 1.6 Hz, 1H), 8.03 (d, *J* = 8.0 Hz, 1H), 7.83 (d, *J* = 8.0 Hz, 1H), 7.66–7.64 (m, 3H), 7.45–7.42 (m, 3H). ESI-MS(+): *m/z* 275.21 [M+H]⁺.

5-((4-Fluorophenyl)ethynyl)-8-nitroquinoline.

Synthesized utilizing Sonogashira coupling method. Product was purified with a gradient of 0–25% EtOAc in hexanes. Isolated as an off-white solid. Yield = 0.17 g (49%). ¹H NMR (CDCl₃, 400 MHz) δ 9.11 (dd, *J*₁ = 4 Hz, *J*₂ = 1.6 Hz, 1H), 8.77 (dd, *J*₁ = 8.0 Hz, *J*₂ = 1.6 Hz, 1H), 8.03 (d, *J* = 8.0 Hz, 1H), 7.82 (d, *J* = 8.0 Hz, 1H), 7.66–7.62 (m, 3H), 7.15–7.11 (m, 2H). ESI-MS(+): *m/z* 293.21 [M+H]⁺.

Protocol for Reduction A —This method was utilized to reduce corresponding nitro compounds into amines, which were utilized in the synthesis of compounds **37-39**, **41-47**, **50-52**, and **55-60**. A solution of 5-Aryl/Cyclic/Ethynyl-8-nitroquinoline in MeOH (25 mL) and Pd/C (10% loading, 0.05 equiv) was degassed for 5–10 mins. The solution mixture was then purged with hydrogen gas (1 atm) and stirred at room temperature for 1–2 hr. The resulting mixture was then filtered through celite and concentrated. The product identity was confirmed via TLC and MS and used in next step without further purification.

Protocol for Reduction B —This method was utilized to reduce corresponding nitro compounds into amines, which were utilized in the synthesis of compounds **40**, **48-49** and **53-54**. To a solution of chlorophenyl-8-nitroquinoline in MeOH:acetone:H₂O (1:1:1, 15 mL) was added K₂CO₃ (4 equiv) and sodium dithionite (4 equiv) then allowed to stir at room temperature under nitrogen overnight. The resulting solution was concentrated to remove organic solvents. The resulting aqueous solution was diluted with water (25 mL) and then extracted with EtOAc (3×50ml). The combined organic fractions were concentrated and to yield product. The product identity was confirmed via TLC and MS and used in next step without further purification.

***N*-(5-Phenylquinolin-8-yl)pyridine-2-sulfonamide (47).**

8-Nitro-5-phenylquinoline was reduced to an amine utilizing Reduction Method A. The corresponding amine was then coupled to pyridine-2-sulfonyl chloride utilizing Sulfonamide Coupling Method A. The product was purified with a gradient of 0–40% EtOAc in hexanes and isolated as a white solid. Yield = 0.115 g (70%). ¹H NMR (CDCl₃, 400 MHz) δ 9.60 (br, 1H), 8.81 (dd, *J*₁ = 4.0 Hz, *J*₂ = 1.6 Hz, 1H), 8.62–8.60 (m, 1H), 8.22 (dd, *J*₁ = 8.4 Hz, *J*₂ = 1.6 Hz, 1H), 8.14 (d, *J* = 8.0 Hz, 1H), 7.97 (d, *J* = 8.0 Hz, 1H), 7.87 (td, *J*₁ = 8.0 Hz, *J*₂ = 1.6 Hz, 1H), 7.49–7.36 (m, 8H). HR-ESI-MS calcd for [C₂₀H₁₆N₃O₂S]⁺: 362.0958; Found: 362.0951.

***N*-(5-(4-Chlorophenyl)quinolin-8-yl)pyridine-2-sulfonamide (48).**

5-(4-Chlorophenyl)-8-nitroquinoline was reduced to an amine utilizing Reduction Method B. The corresponding amine was then coupled to pyridine-2-sulfonyl chloride utilizing Sulfonamide Coupling Method A. The product was purified with a gradient of 0–40% EtOAc in hexanes and isolated as a white solid. Yield = 0.061 g (79%). ¹H NMR (CDCl₃, 400 MHz) δ 9.60 (br, 1H), 8.80 (dd, *J*₁ = 4.0 Hz, *J*₂ = 1.6 Hz, 1H), 8.60 (dd, *J*₁ = 8.0 Hz, *J*₂ = 1.6 Hz, 1H), 8.15 (m, 2H), 7.96 (d, *J* = 8.0 Hz, 1H), 7.87 (td, *J*₁ = 8.0 Hz, *J*₂ = 1.6 Hz, 1H), 7.44–7.29 (m, 7H). HR-ESI-MS calcd for [C₂₀H₁₅ClN₃O₂S]⁺: 396.0568; Found: 396.0563.

***N*-(5-(3-Chlorophenyl)quinolin-8-yl)pyridine-2-sulfonamide (49).**

5-(3-Chlorophenyl)-8-nitroquinoline was reduced to an amine utilizing Reduction Method B. The corresponding amine was then coupled to pyridine-2-sulfonyl chloride utilizing Sulfonamide Coupling Method A. The product was purified with a gradient of 0–50% EtOAc in hexanes and isolated as a light pink solid. Yield = 0.05 g (16%). ¹H NMR (CDCl₃, 400 MHz) δ 9.60 (br, 1H), 8.82–8.80 (m, 1H), 8.61 (dd, *J*₁ = 8.0 Hz, *J*₂ = 1.6 Hz, 1H), 8.17–8.12 (m, 2H), 7.97 (d, *J* = 8.0 Hz, 1H), 7.87 (td, *J*₁ = 8.0 Hz, *J*₂ = 1.6 Hz, 1H), 7.43–7.32 (m, 6H), 7.18 (t, *J* = 8.0 Hz, 1H). HR-ESI-MS calcd for [C₂₀H₁₅ClN₃O₂S]⁺: 396.0568; Found: 396.0565.

***N*-(5-(4-Fluorophenyl)quinolin-8-yl)pyridine-2-sulfonamide (50).**

5-(4-Fluorophenyl)-8-nitroquinoline was reduced to an amine utilizing Reduction Method A. The corresponding amine was then coupled to pyridine-2-sulfonyl chloride utilizing Sulfonamide Coupling Method A. The product was purified with a gradient of 0–45% EtOAc in hexanes and isolated as a light yellow solid. Yield = 0.091 g (36%). ¹H NMR (CDCl₃, 400 MHz) δ 9.59 (br, 1H), 8.80–8.79 (m, 1H), 8.60 (dd, *J*₁ = 8.0 Hz, *J*₂ = 1.6 Hz, 1H), 8.15–8.11 (m, 2H), 7.97 (d, *J* = 8.0 Hz, 1H), 7.88 (td, *J*₁ = 8.0 Hz, *J*₂ = 1.6 Hz, 1H), 7.44–7.31 (m, 5H), 7.17–7.13 (m, 2H). HR-ESI-MS calcd for [C₂₀H₁₅FN₃O₂S]⁺: 380.0864; Found: 380.0866.

***N*-(5-(4-Methoxyphenyl)quinolin-8-yl)pyridine-2-sulfonamide (51).**

5-(4-Methoxyphenyl)-8-nitroquinoline was reduced to an amine utilizing Reduction Method A. The corresponding amine was then coupled to pyridine-2-sulfonyl chloride utilizing Sulfonamide Coupling Method A. The product was purified with a gradient of 0–50% EtOAc in hexanes and isolated as a white solid. Yield = 0.12 g (43%). ¹H NMR (CDCl₃, 400 MHz) δ 9.60 (br, 1H), 8.80–8.79 (m, 1H), 8.61–8.60 (m, 1H), 8.25 (dd, *J*₁ = 8.0 Hz, *J*₂ = 1.6 Hz, 1H), 8.14 (dd, *J*₁ = 4.0 Hz, *J*₂ = 0.8 Hz, 1H), 7.97 (d, *J* = 8.0 Hz, 1H), 7.88 (td, *J*₁ = 8.0 Hz, *J*₂ = 1.6 Hz, 1H), 7.42–7.35 (m, 4H), 6.97–6.91 (m, 3H). HR-ESI-MS calcd for [C₂₁H₁₈N₃O₃S]⁺: 392.1063; Found: 392.1061.

***N*-(5-(3-Methoxyphenyl)quinolin-8-yl)pyridine-2-sulfonamide (52).**

5-(3-Methoxyphenyl)-8-nitroquinoline was reduced to an amine utilizing Reduction Method A. The corresponding amine was then coupled to pyridine-2-sulfonyl chloride utilizing Sulfonamide Coupling Method A. The product was purified with a gradient of 0–100% EtOAc in hexanes and isolated as a white solid. Yield = 0.074 g (21%). ¹H NMR (CDCl₃, 400 MHz) δ 9.59 (br, 1H), 8.79 (dd, *J*₁ = 4.0 Hz, *J*₂ = 1.6 Hz, 1H), 8.61–8.59 (m, 1H), 8.22 (dd, *J*₁ = 8.0 Hz, *J*₂ = 1.6 Hz, 1H), 8.13–8.11 (m, 1H), 7.95 (d, *J* = 8.0 Hz, 1H), 7.86 (td, *J*₁ = 8.0 Hz, *J*₂ = 1.6 Hz, 1H), 7.41–7.29 (m, 5H), 7.01–6.00 (m, 2H). HR-ESI-MS calcd for [C₂₁H₁₈N₃O₃S]⁺: 392.1063; Found: 392.1065.

***N*-(5-(3-Chloro-4-methoxyphenyl)quinolin-8-yl)pyridine-2-sulfonamide (53).**

5-(3-Chloro-4-methoxyphenyl)-8-nitroquinoline was reduced to an amine utilizing Reduction Method B. The corresponding amine was then coupled to pyridine-2-sulfonyl chloride utilizing Sulfonamide Coupling Method A. The product was purified with a

gradient of 0–100% EtOAc in hexanes and isolated as a white solid. Yield = 0.15 g (51%). ¹H NMR (CDCl₃, 400 MHz) δ 9.59 (br, 1H), 8.82 (dd, *J*₁ = 4.4 Hz, *J*₂ = 2.0 Hz, 1H), 8.61–8.60 (m, 1H), 8.19 (dd, *J*₁ = 8.4 Hz, *J*₂ = 2.0 Hz, 1H), 8.13 (d, *J* = 8.0 Hz, 1H), 7.96 (d, *J* = 8.0 Hz, 1H), 7.88 (td, *J*₁ = 8.0 Hz, *J*₂ = 1.6 Hz, 1H), 7.43–7.39 (m, 3H), 7.36 (d, *J* = 8.0 Hz, 1H), 7.26 (dd, *J*₁ = 8.4 Hz, *J*₂ = 2.0 Hz, 1H), 7.04 (d, *J* = 8.4 Hz, 1H), 3.97 (s, 3H). HR-ESI-MS calcd for [C₂₁H₁₆ClN₃NaO₃S]⁺: 448.0493; Found: 448.0491.

***N*-(5-(3,4-Dichlorophenyl)quinolin-8-yl)pyridine-2-sulfonamide (54).**

5-(3,4-Dichlorophenyl)-8-nitroquinoline was reduced to an amine utilizing Reduction Method B. The corresponding amine was then coupled to pyridine-2-sulfonyl chloride utilizing Sulfonamide Coupling Method A. The product was purified with a gradient of 0–100% EtOAc in hexanes and isolated as a white solid. Yield = 0.17 g (58%). ¹H NMR (CDCl₃, 400 MHz) δ 9.61 (br, 1H), 8.85 (dd, *J*₁ = 4.4 Hz, *J*₂ = 2.0 Hz, 1H), 8.62–8.60 (m, 1H), 8.15–8.12 (m, 2H), 7.99 (d, *J* = 8.0 Hz, 1H), 7.89 (td, *J*₁ = 8.0 Hz, *J*₂ = 1.6 Hz, 1H), 7.56–7.35 (m, 5H), 7.23 (m, 1H). HR-ESI-MS calcd for [C₂₀H₁₄Cl₂N₃O₂S]⁺: 430.0178; Found: 430.0180.

***N*-(5-(3,5-Dimethoxyphenyl)quinolin-8-yl)pyridine-2-sulfonamide (55).**

5-(3,5-Dimethoxy phenyl)-8-nitroquinoline was reduced to an amine utilizing Reduction Method A. The corresponding amine was then coupled to pyridine-2-sulfonyl chloride utilizing Sulfonamide Coupling Method A. The product was purified with a gradient of 0–100% EtOAc in hexanes and isolated as an off-white solid. Yield = 0.145 g (56%). ¹H NMR (CDCl₃, 400 MHz) δ 9.58 (br, 1H), 8.77–8.75 (m, 1H), 8.58–8.57 (m, 1H), 8.26 (dd, *J*₁ = 8.0 Hz, *J*₂ = 1.6 Hz, 1H), 8.12 (dd, *J*₁ = 8.0 Hz, *J*₂ = 0.8 Hz, 1H), 7.94 (dd, *J*₁ = 8.0 Hz, *J*₂ = 1.6 Hz, 1H), 7.86 (td, *J*₁ = 8.0 Hz, *J*₂ = 1.6 Hz, 1H), 7.41–7.34 (m, 3H), 6.50 (m, 3H), 3.79 (s, 6H). HR-ESI-MS calcd for [C₂₂H₂₀N₃O₄S]⁺: 422.1169; Found: 422.1165.

***N*-(5-Phenethylquinolin-8-yl)pyridine-2-sulfonamide (56).**

8-Nitro-5-(phenylethynyl) quinoline was reduced to an amine utilizing Reduction Method A. The corresponding amine was then coupled to pyridine-2-sulfonyl chloride utilizing Sulfonamide Coupling Method A. The product was purified with a gradient of 0–100% EtOAc in hexanes and isolated as an off-white solid. Yield = 0.045 g (15%). ¹H NMR (CDCl₃, 400 MHz) δ 9.51 (br, 1H), 8.77 (d, *J* = 2.4 Hz, 1H), 8.57 (d, *J* = 3.6 Hz, 1H), 8.27 (d, *J* = 8.4 Hz, 1H), 8.07 (d, *J* = 8.4 Hz, 1H), 7.82–7.81 (m, 2H), 7.42–7.11 (m, 8H), 3.23 (t, *J* = 8.4 Hz, 2H), 2.95 (t, *J* = 8.4 Hz, 2H). HR-ESI-MS calcd for [C₂₂H₂₀N₃O₂S]⁺: 390.1271; Found: 390.1265.

***N*-(5-(4-Fluorophenethyl)quinolin-8-yl)pyridine-2-sulfonamide (57).**

5-((4-Fluorophenyl) ethynyl)-8-nitroquinoline was reduced to an amine utilizing Reduction Method A. The corresponding amine was then coupled to pyridine-2-sulfonyl chloride utilizing Sulfonamide Coupling Method A. The product was purified with a gradient of 0–100% EtOAc in hexanes and isolated as an off-white solid. Yield = 0.07 g (31%). ¹H NMR (CDCl₃, 400 MHz) δ 9.50 (br, 1H), 8.75 (d, *J* = 2.4 Hz, 1H), 8.56 (d, *J* = 3.6 Hz, 1H), 8.24 (d, *J* = 8.4 Hz, 1H), 8.07 (d, *J* = 8.4 Hz, 1H), 7.83–7.78 (m, 2H), 7.43–7.35 (m, 2H), 7.17 (d,

$J = 8.4$ Hz, 1H), 7.03–7.00 (m, 2H), 6.92 (m, 2H), 3.21 (t, $J = 8.4$ Hz, 2H), 2.92 (t, $J = 8.4$ Hz, 2H). HR-ESI-MS calcd for $[C_{22}H_{18}FN_3NaO_2S]^+$: 430.0996; Found: 430.0994.

6-Bromo-8-nitroquinoline.

A solution of 4-bromo-2-nitroaniline (5 g, 23.04 mmol) in toluene (30 mL) and 6M HCl (30 mL) was heated to reflux for ~15 min. To this was added acrolein (1.93 g, 34.6 mmol) and allowed to heat at reflux for an additional 2 h. The resulting solution was then partitioned, and the organic layer was discarded. The aqueous layer was made strongly basic (pH 10–11) with 6M NaOH. The resulting basic mixture was then extracted with EtOAc (3×50mL). The combined organic layers were dried over $MgSO_4$, filtered, concentrated then purified via silica gel chromatography eluting 0–40% EtOAc in hexanes. The desired product was isolated as a pink-orange solid. Yield = 1.21 g (21%). 1H NMR ($CDCl_3$, 400 MHz) δ 9.08 (dd, $J_1 = 4.0$ Hz, $J_2 = 1.6$ Hz, 1H), 8.20–8.18 (m, 2H), 8.13 (d, $J_1 = 2.4$ Hz, 1H), 7.60 (dd, $J_1 = 8.4$ Hz, $J_2 = 4$ Hz, 1H). ESI-MS(+): m/z 253.19 $[M+H]^+$.

8-Nitro-6-(phenylethynyl)quinoline.

Synthesized utilizing Sonogashira coupling method. The product was purified with a gradient of 0–100% EtOAc in hexanes and isolated as an off-white solid. Yield = 0.12 g (40%). 1H NMR ($CDCl_3$, 400 MHz) δ 9.00 (dd, $J_1 = 4.4$ Hz, $J_2 = 1.6$ Hz, 1H), 8.20–8.09 (m, 3H), 7.56–7.51 (m, 3H), 7.38–7.36 (m, 3H). ESI-MS(+): m/z 275.21 $[M+H]^+$.

6-((4-Fluorophenyl)ethynyl)-8-nitroquinoline.

Synthesized utilizing Sonogashira coupling method. The product was purified with a gradient of 0–100% EtOAc in hexanes and isolated as an off-white solid. Yield = 0.15 g (50%). 1H NMR ($CDCl_3$, 400 MHz) δ 9.11 (dd, $J_1 = 4.0$ Hz, $J_2 = 1.6$ Hz, 1H), 8.33–8.03 (m, 3H), 7.80–7.61 (m, 2H), 7.37–7.36 (m, 3H). ESI-MS(+): m/z 293.11 $[M+H]^+$.

6-((3,5-Dimethoxyphenyl)ethynyl)-8-nitroquinoline.

Synthesized utilizing Sonogashira coupling method. The product was purified with a gradient of 0–100% EtOAc in hexanes and isolated as a tan solid. Yield = 0.29 g (73%). 1H NMR ($CDCl_3$, 400 MHz) δ 9.07 (dd, $J_1 = 4.0$ Hz, $J_2 = 1.6$ Hz, 1H), 8.24 (dd, $J_1 = 4.0$ Hz, $J_2 = 1.6$ Hz, 1H), 8.19–8.15 (m, 2H), 7.60 (dd, $J_1 = 8.4$ Hz, $J_2 = 4.4$ Hz, 1H), 6.73 (d, $J = 2.4$ Hz), 6.53 (t, $J = 2.4$ Hz), 3.82 (s, 6H). ESI-MS(+): m/z 335.33 $[M+H]^+$.

N-(6-Phenethylquinolin-8-yl)pyridine-2-sulfonamide (58).

8-Nitro-6-(phenylethynyl) quinoline was reduced to an amine utilizing Reduction Method A. The corresponding amine was then coupled to pyridine-2-sulfonyl chloride utilizing Sulfonamide Coupling Method A. The product was purified with a gradient of 0–100% EtOAc in hexanes and isolated as an off-white solid. Yield = 0.065 g (35%). 1H NMR ($CDCl_3$, 400 MHz) δ 9.48 (br, 1H), 8.71 (d, $J = 4.4$ Hz, 1H), 8.56 (d, $J = 4.4$ Hz, 1H), 8.06 (d, $J = 8.0$ Hz, 1H), 7.97 (d, $J = 8.0$ Hz, 1H), 7.85–7.77 (m, 2H), 7.37–7.34 (m, 2H), 7.24–7.11 (m, 7H), 3.05 (t, $J = 8.4$ Hz, 2H), 2.96 (t, $J = 8.4$ Hz, 2H). HR-ESI-MS calcd for $[C_{22}H_{20}N_3O_2S]^+$: 390.1271; Found: 390.1268.

N-(6-(4-Fluorophenyl)quinolin-8-yl)pyridine-2-sulfonamide (59).

6-((4-Fluorophenyl) ethynyl)-8-nitroquinoline was reduced to an amine utilizing Reduction Method A. The corresponding amine was then coupled to pyridine-2-sulfonyl chloride utilizing Sulfonamide Coupling Method A. The product was purified with a gradient of 0–100% EtOAc in hexanes and isolated as an off-white solid. Yield = 0.075 g (36%). ¹H NMR (CDCl₃, 400 MHz) δ 9.45 (br, 1H), 8.72 (d, *J* = 4.4 Hz, 1H), 8.56 (d, *J* = 4.4 Hz, 1H), 8.05 (d, *J* = 8.0 Hz, 1H), 7.98 (d, *J* = 8.0 Hz, 1H), 7.82–7.78 (m, 2H), 7.39–7.36 (m, 2H), 7.13 (s, 1H), 7.04–7.01 (m, 2H), 6.91–6.87 (m, 2H), 3.02 (t, *J* = 8.4 Hz, 2H), 2.94 (t, *J* = 8.4 Hz, 2H). HR-ESI-MS calcd for [C₂₂H₁₈FN₃NaO₂S]⁺: 430.0996; Found: 430.0994.

N-(6-(3,5-Dimethoxyphenyl)quinolin-8-yl)pyridine-2-sulfonamide (60).

6-((3,5-Dimethoxyphenyl)ethynyl)-8-nitroquinoline was reduced to an amine utilizing Reduction Method A. The corresponding amine was then coupled to pyridine-2-sulfonyl chloride utilizing Sulfonamide Coupling Method A. The product was purified with a gradient of 0–100% EtOAc in hexanes and isolated as an off-white solid. Yield = 0.165 g (45%). ¹H NMR (CDCl₃, 400 MHz) δ 9.50 (br, 1H), 8.73 (d, *J* = 4.4 Hz, 1H), 8.57 (d, *J* = 4.4 Hz, 1H), 8.07 (d, *J* = 8.0 Hz, 1H), 8.02 (d, *J* = 8.0 Hz, 1H), 7.87 (s, 1H), 7.83 (td, *J*₁ = 8.0 Hz, *J*₂ = 1.6 Hz, 1H), 7.41–7.35 (m, 2H), 7.21 (s, 1H), 6.32 (s, 3H), 3.74 (s, 6H), 3.06 (t, *J* = 8.4 Hz, 2H), 2.92 (t, *J* = 8.4 Hz, 2H). HR-ESI-MS calcd for [C₂₄H₂₄N₃O₄S]⁺: 450.1482; Found: 450.1483.

Human Glyoxalase 1 Assay.

Recombinant human glyoxalase I (GLO1) was purchased from R&D Systems (Catalog #4959-GL). Assays were carried out in 100 mM sodium phosphate, pH 7.0 buffer, utilizing 96-well Clear UV Plate (Corning UV Transparent Microplates, Catalog #3635). A fresh solution of glutathione (GSH, 100 mM) and methylglyoxal (MG, 100 mM) was prepared in Millipore grade water. The substrate for the assay was prepared by adding 0.99 mL of GSH and 0.99 mL of MG to 14.5 mL of buffer. The substrate mixture was vortexed vigorously for 15 sec, then allowed to sit at room temperature for 20 min. The initial well volume was 50 μL containing GLO1 (40 ng) and inhibitor. This protein and inhibitor mixture was incubated for 15–20 min prior to addition of substrate. Substrate (150 μL) was then added to the wells yielding a maximum amount of 5% DMSO per well. The enzyme activity was measured utilizing a Biotek Synergy HT or H4 plate reader by measuring absorbance at 240 nm every 1 min for a duration of 8 min. The rate of absorbance increase was compared for samples versus controls containing no inhibitor (set at 100% activity). The absorbance reading for background wells containing DMSO, buffer, and substrate (no enzyme or inhibitor) were subtracted from the experimental wells. All IC₅₀ values were benchmarked against a positive control compound **Chugai-1** (1-hydroxy-4,6-diphenylpyridin-2(1*H*)-one). **Chugai-1** was prepared and evaluated under the assay conditions described above gave an IC₅₀ value of 1.9±0.2 μM, which is comparable to the value reported in the original literature report (1.19 μM).²⁸

Molecular Modeling.

Modeling studies were performed using the Molecular Operating Environment (MOE) 2014 software suite. The glyoxalase crystal structure titled “*Human Glyoxalase I with an N-hydroxypyridone inhibitor*” with PDB ID 3VW9 was obtained from the Protein Data Bank.²⁸ The PDB ID 3VW9 crystal structure was utilized because the **Chugai-3d** inhibitor utilizes bidentate metal binding to the GLO1 active site Zn(II) ion, which is also the anticipated binding mode for **8-MSQ** and its derivatives. In addition, **Chugai-3d** has several substituents that result in tight binding to GLO1, which can be used as a guide for designing suitable substituents for appending to **8-MSQ**. A binding model for **8-MSQ** and its analogs was obtained through visual positioning of the fragment into the GLO1 active site and superimposing the coordinating atoms (*N, N*) of **8-MSQ** with those of the bound **Chugai-3d** inhibitor (*O, O*). The bound Chugai-3d inhibitor was then removed from the structure and replaced with **8-MSQ** (or the appropriate **8-MSQ** derivative, Figures S1-S4), which then utilized the position of the metal-coordinating donor atoms of the **Chugai-3d** inhibitor as an initial guide for the binding mode of **8-MSQ** and its derivatives. Once **8-MSQ** was modeled in, the “builder” tool of MOE was utilized to introduce substituents to the bound **8-MSQ** fragment. Substituents were built onto the bound **8-MSQ** fragment and inspected via the “contacts/clash” visualizing tool of MOE. The substituents were freely rotated and manually moved to generate interactions while avoiding clashes as predicted by MOE. By building in functional groups to **8-MSQ** and visually inspecting the protein active site, it allowed for a hypothesis to be generated and predictions for which substituents were sterically tolerated, as well as which substituents could form interactions within the protein active site. The protein structure was not minimized or altered in any way during these modeling exercises. PDB files for all modeled compounds have been provided as part of the Supporting Information.

Animal Subjects.

Male and female FVB/NJ mice ($n=21$) were bred in house at U.C. San Diego and were housed 2–5 per cage on Sani-Chip bedding with food (Envigo 8604; Indianapolis, IN) and water given *ad libitum*. All animals were between 108 and 148 days old at the start of testing. Mice were housed on a 12h/12h light-dark cycle with lights on at 06:00, and all behavioral testing occurred during the light phase. All procedures were approved by the local Institutional Animal Care and Use Committee and were conducted in accordance with the NIH Guidelines for the Care and Use of Laboratory Animals.

Forced Swim Test (FST).

The forced swim test procedure was based on protocols used previously by our laboratory and others to test GLO1 inhibitors and classical antidepressants for their ability to reduce depression-like behavior.^{41,46} Briefly, mice were placed into white opaque plastic buckets (61 cm high, 48 cm diameter) filled 48 cm high with 23–25 tap water for 6 min. Test sessions were videotaped by a camera positioned directly above swim buckets. An experimenter blind to treatment scored the last 4 min of each video for time spent immobile, which is a measure of depression-like behavior and is reduced by antidepressant treatment.

Open Field Test.

Locomotor behavior was measured using an open field test, which has been described previously.⁴⁷ Briefly, mice were placed in the center of a square chamber (43×43×33 cm, Accusan, Columbus, OH) with dim overhead lighting inside of sound- and light-attenuating boxes and allowed to freely explore for 30 min. A grid of infrared detection beams in each chamber and Versamax software was used to track animal location and locomotor activity (distance traveled) during the test.

Determination of 60 and MG in Mouse Brain Tissue.

Mice were anesthetized with isoflurane, the chest cavity opened to expose the pulsating heart, and a 25 gauge butterfly needle attached to a 25 mL syringe filled with PBS inserted into the left ventricle. The right atrium was then cut to allow outflow of systemic blood, then PBS slowly infused into the heart to purge residual systemic blood over approximately 20 min. When liver and kidneys were pale in color, the brain was removed, weighed, placed in a polypropylene tube and flash frozen in liquid nitrogen, and then stored at -80 °C. For quantitative analysis of each probe compound in brain, whole mouse brains were minced (~20 mg per piece), then extracted with acetonitrile, homogenized using a bead beater, and centrifuged at 5000 rpm for 5 min. The supernatant was collected and filtered through a 2 µm filter to remove any residual particulate matter. Determination of 60 and MG in brain extracts was performed with liquid chromatography-tandem mass spectrometry (LC-MS/MS). Eleven-point calibration curves, ranging between 5 – 5000 ng/mL, were constructed for each analyte by spiking a known amount of each compound into blank matrix (untreated mouse brain) and used as the basis to determine unknown concentrations. Results were normalized to wet weight of brain tissue (i.e., ng/mg of brain tissue).

Supplementary Material

Refer to Web version on PubMed Central for supplementary material.

Acknowledgements

The authors acknowledge Dr. Yongxuan Su (U.C. San Diego, Molecular Mass Spectrometry Facility) for aid with HR-MS and HPLC compound purity analysis. This work was supported by grants from the National Institutes of Health (R01 GM098435 to S.M.C.; F32AA025515 to A.M.B-L.). B.L.D. was supported by the National Institute of Health Molecular Biophysics Training Grant (T32GM008326-26). S.M.C. is a co-founder, has an equity interest, and receives income as member of the Scientific Advisory Board for Cleave Biosciences and is a co-founder, has an equity interest, and a member of the Scientific Advisory Board for Forge Therapeutics. Both companies may potentially benefit from the research results of certain projects in the laboratory of S.M.C. The terms of this arrangement have been reviewed and approved by the University of California, San Diego in accordance with its conflict of interest policies.

List of Abbreviations

FBDD	fragment-based drug discovery
FST	forced swim test
GLO1	glyoxalase 1
GLO2	glyoxalase 2

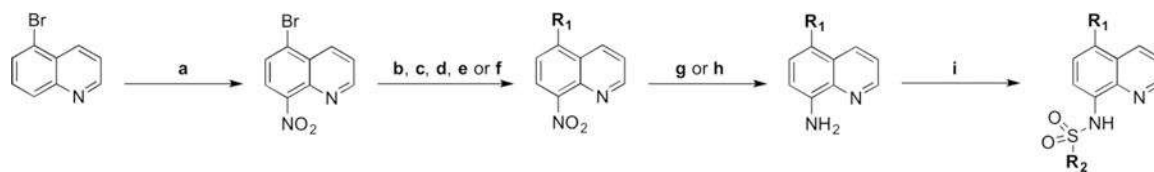
GSH	glutathione
MBP	metal-binding pharmacophore
MG	methylglyoxal
MSQ-8	8-(methylsulfonylamino)quinoline

REFERENCES

- (1). Baxter AJ; Vos T; Scott KM; Ferrari AJ; Whiteford HA The Global Burden of Anxiety Disorders in 2010. *Psychol. Med* 2014, 44, 2363–2374. [PubMed: 24451993]
- (2). Machado-Vieira R; Henter ID; Zarate CA Jr. New Targets for Rapid Antidepressant Action. *Prog. Neurobiol* 2017, 152, 21–37. [PubMed: 26724279]
- (3). Thornalley PJ The Glyoxalase System in Health and Disease. *Mol. Aspects Med* 1993, 14, 287–371. [PubMed: 8277832]
- (4). Thornalley PJ The Glyoxalase System: New Developments Towards Functional Characterization of a Metabolic Pathway Fundamental to Biological Life. *Biochem. J* 1990, 269, 1–11. [PubMed: 2198020]
- (5). Mannervik B Molecular Enzymology of the Glyoxalase System. *Drug Metab. Drug Interact* 2008, 23, 13–27.
- (6). Thornalley PJ Protecting the Genome: Defence Against Nucleotide Glycation and Emerging Role of Glyoxalase I Overexpression in Multidrug Resistance in Cancer Chemotherapy. *Biochem. Soc. Trans* 2003, 31, 1372–1377. [PubMed: 14641066]
- (7). Brownlee M Biochemistry and Molecular Cell Biology of Diabetic Complications. *Nature* 2001, 414, 813–820. [PubMed: 11742414]
- (8). Schleicher E; Friess U Oxidative Stress, AGE, and Atherosclerosis. *Kidney Int. Suppl* 2007, S17–26. [PubMed: 17653206]
- (9). Loh KP; Huang SH; De Silva R; Tan BK; Zhu YZ Oxidative Stress: Apoptosis in Neuronal Injury. *Curr. Alzheimer Res* 2006, 3, 327–337. [PubMed: 17017863]
- (10). Sousa Silva M; Gomes RA; Ferreira AE; Ponces Freire A; Cordeiro C The Glyoxalase Pathway: The First Hundred Years... and Beyond. *Biochem. J* 2013, 453, 1–15. [PubMed: 23763312]
- (11). Creighton DJ; Zheng ZB; Holewinski R; Hamilton DS; Eiseman JL Glyoxalase I Inhibitors in Cancer Chemotherapy. *Biochem. Soc. Trans* 2003, 31, 1378–1382. [PubMed: 14641067]
- (12). Thornalley PJ Advances in Glyoxalase Research. Glyoxalase Expression in Malignancy, Anti-proliferative Effects of Methylglyoxal, Glyoxalase I Inhibitor Diesters and S-D-lactoylglutathione, and Methylglyoxal-Modified Protein Binding and Endocytosis by the Advanced Glycation Endproduct Receptor. *Crit. Rev. Oncol. Hematol* 1995, 20, 99–128. [PubMed: 7576201]
- (13). Benton CS; Miller BH; Skwerer S; Suzuki O; Schultz LE; Cameron MD; Marron JS; Pletcher MT; Wiltshire T Evaluating Genetic Markers and Neurobiochemical Analytes for Fluoxetine Response Using a Panel of Mouse Inbred Strains. *Psychopharmacology* 2012, 221, 297–315. [PubMed: 22113448]
- (14). Distler MG; Palmer AA Role of Glyoxalase 1 (Glo1) and Methylglyoxal (MG) in Behavior: Recent Advances and Mechanistic Insights. *Front. Genet* 2012, 3, 250. [PubMed: 23181072]
- (15). Distler MG; Plant LD; Sokoloff G; Hawk AJ; Aneas I; Wuenschell GE; Termini J; Meredith SC; Nobrega MA; Palmer AA Glyoxalase 1 Increases Anxiety by Reducing GABAA Receptor Agonist Methylglyoxal. *J. Clin. Invest* 2012, 122, 2306–2315. [PubMed: 22585572]
- (16). Hovatta I; Tennant RS; Helton R; Marr RA; Singer O; Redwine JM; Ellison JA; Schadt EE; Verma IM; Lockhart DJ; Barlow C Glyoxalase 1 and Glutathione Reductase 1 Regulate Anxiety in Mice. *Nature* 2005, 438, 662–666. [PubMed: 16244648]
- (17). Loos M; van der Sluis S; Bochdanovits Z; van Zutphen IJ; Pattij T; Stiedl O; Neuro B. M. P. c.; Smit AB; Spijker S. Activity and Impulsive Action are Controlled by Different Genetic and Environmental Factors. *Genes, Brain Behav* 2009, 8, 817–828. [PubMed: 19751396]

- (18). Al-Balas QA; Hassan MA; Al-Shar'i NA; Al-Jabal GA; Almaaytah AM Recent Advances in Glyoxalase-I Inhibition. *Mini-Rev. Med. Chem* 2019, 19, 281–291. [PubMed: 30306863]
- (19). Murthy NSRK; Bakeris T; Kavarana MJ; Hamilton DS; Lan Y; Creighton DJ S-(N-Aryl-N-hydroxycarbamoyl)glutathione Derivatives Are Tight-Binding Inhibitors of Glyoxalase I and Slow Substrates for Glyoxalase II. *J. Med. Chem* 1994, 37, 2161–2166. [PubMed: 8035422]
- (20). Sharkey EM; O'Neill HB; Kavarana MJ; Wang HB; Creighton DJ; Sentz DL; Eiseman JL Pharmacokinetics and Antitumor Properties in Tumor-bearing Mice of an Eneiol Analogue Inhibitor of Glyoxalase I. *Cancer Chemother. Pharmacol* 2000, 46, 156–166. [PubMed: 10972486]
- (21). Yuan MG; Luo MX; Song Y; Xu Q; Wang XF; Cao Y; Bu XZ; Ren YL; Hu XP Identification of Curcumin Derivatives as Human Glyoxalase I Inhibitors: A Combination of Biological Evaluation, Molecular Docking, 3D-QSAR and Molecular Dynamics Simulation Studies. *Bioorg. Med. Chem* 2011, 19, 1189–1196. [PubMed: 21237663]
- (22). Liu M; Yuan MG; Luo MX; Bu XZ; Luo HB; Hu XP Binding of Curcumin with Glyoxalase I: Molecular Docking, Molecular Dynamics Simulations, and Kinetics Analysis. *Biophys. Chem* 2010, 147, 28–34. [PubMed: 20071071]
- (23). Zhang H; Zhai J; Zhang LP; Li CY; Zhao YN; Chen YY; Li Q; Hu XP In Vitro Inhibition of Glyoxalase I by Flavonoids: New Insights from Crystallographic Analysis. *Curr. Top. Med. Chem* 2016, 16, 460–466. [PubMed: 26268338]
- (24). Al-Balas QA; Hassan MA; Al-Shar'i NA; Mhaidat NM; Almaaytah AM; Al-Mahasneh FM; Isawi IH Novel Glyoxalase-I Inhibitors Possessing a “Zinc-binding Feature” as Potential Anticancer Agents. *Drug Des. Dev. Ther* 2016, 10, 2623–2629.
- (25). Yadav A; Kumar R; Sunkaria A; Singhal N; Kumar M; Sandhir R Evaluation of Potential Flavonoid Inhibitors of Glyoxalase-I Based on Virtual Screening and in Vitro Studies. *J. Biomol. Struct. Dyn* 2016, 34, 993–1007. [PubMed: 26108947]
- (26). Kawatani M; Okumura H; Honda K; Kanoh N; Muroi M; Dohmae N; Takami M; Kitagawa M; Futamura Y; Imoto M; Osada H The Identification of an Osteoclastogenesis Inhibitor Through the Inhibition of Glyoxalase I. *Proc. Natl. Acad. Sci. U. S. A* 2008, 105, 11691–11696. [PubMed: 18695250]
- (27). Santel T; Pflug G; Hemdan NYA; Schafer A; Hollenbach M; Buchold M; Hintersdorf A; Lindner I; Otto A; Bigl M; Oerlecke I; Hutschenreuter A; Sack U; Huse K; Groth M; Birkemeyer C; Schellenberger W; Gebhardt R; Platzer M; Weiss T; Vijayalakshmi MA; Kruger M; Birkenmeier G Curcumin Inhibits Glyoxalase 1-A Possible Link to Its Anti-Inflammatory and Anti-Tumor Activity. *PLOS One* 2008, 3, e3508. [PubMed: 18946510]
- (28). Chiba T; Ohwada J; Sakamoto H; Kobayashi T; Fukami TA; Irie M; Miura T; Ohara K; Koyano H Design and Evaluation of Azaindole-substituted N-Hydroxypyridones as Glyoxalase I Inhibitors. *Bioorg. Med. Chem. Lett* 2012, 22, 7486–7489. [PubMed: 23122816]
- (29). Joseph-McCarthy D; Campbell AJ; Kern G; Moustakas D Fragment-based Lead Discovery and Design. *J. Chem. Inf. Model* 2014, 54, 693–704. [PubMed: 24490951]
- (30). Jacobsen JA; Fullagar JL; Miller MT; Cohen SM Identifying Chelators for Metalloprotein Inhibitors Using a Fragment-based Approach. *J. Med. Chem* 2011, 54, 591–602. [PubMed: 21189019]
- (31). Perez C; Li J; Parlati F; Rouffet M; Ma Y; Mackinnon AL; Chou TF; Deshaies RJ; Cohen SM Discovery of an Inhibitor of the Proteasome Subunit Rpn11. *J. Med. Chem* 2017, 60, 1343–1361. [PubMed: 28191850]
- (32). Credille CV; Chen Y; Cohen SM Fragment-Based Identification of Influenza Endonuclease Inhibitors. *J. Med. Chem* 2016, 59, 6444–6454. [PubMed: 27291165]
- (33). Fullagar JL; Garner AL; Struss AK; Day JA; Martin DP; Yu J; Cai X; Janda KD; Cohen SM Antagonism of a Zinc Metalloprotease Using a Unique Metal-chelating Scaffold: Tropolones as Inhibitors of *P. Aeruginosa* Elastase. *ChemComm* 2013, 49, 3197–3199.
- (34). Garner AL; Struss AK; Fullagar JL; Agrawal A; Moreno AY; Cohen SM; Janda KD 3-Hydroxy-1-alkyl-2-methylpyridine-4(1H)-thiones: Inhibition of the *Pseudomonas Aeruginosa* Virulence Factor LasB. *ACS Med. Chem. Lett* 2012, 3, 668–672.

- (35). Arai M; Nihonmatsu-Kikuchi N; Itokawa M; Rabbani N; Thornalley PJ Measurement of Glyoxalase Activities. *Biochem. Soc. Trans* 2014, 42, 491–494. [PubMed: 24646266]
- (36). Fahrni CJ; O'Halloran TV Aqueous Coordination Chemistry of Quinoline-based Fluorescence Probes for the Biological Chemistry of Zinc. *J. Am. Chem. Soc* 1999, 121, 11448–11458.
- (37). Taki M; Wolford JL; O'Halloran TV Emission Ratiometric Imaging of Intracellular Zinc: Design of a Benzoxazole Fluorescent Sensor and Its Application in Two-photon Microscopy. *J. Am. Chem. Soc* 2004, 126, 712–713. [PubMed: 14733534]
- (38). Rouffet M; de Oliveira CA; Udi Y; Agrawal A; Sagi I; McCammon JA; Cohen SM From Sensors to Silencers: Quinoline- and Benzimidazole-sulfonamides as Inhibitors for Zinc Proteases. *J. Am. Chem. Soc* 2010, 132, 8232–8233. [PubMed: 20507095]
- (39). Chai SC; Ye QZ Metal-mediated Inhibition is a Viable Approach for Inhibiting Cellular Methionine Aminopeptidase. *Bioorg. Med. Chem. Lett* 2009, 19, 6862–6864. [PubMed: 19889537]
- (40). Ramaker MJ; Dulawa SC Identifying Fast-onset Antidepressants Using Rodent Models. *Mol. Psychiatry* 2017, 22, 656–665. [PubMed: 28322276]
- (41). McMurray KMJ; Ramaker MJ; Barkley-Levenson AM; Sidhu PS; Elkin PK; Reddy MK; Guthrie ML; Cook JM; Rawal VH; Arnold LA; Dulawa SC; Palmer AA Identification of a Novel, Fast-acting GABAergic Antidepressant. *Mol. Psychiatry* 2018, 23, 384–391. [PubMed: 28322281]
- (42). Baell JB; Holloway GA New Substructure Filters for Removal of Pan Assay Interference Compounds (PAINS) from Screening Libraries and for Their Exclusion in Bioassays. *J. Med. Chem* 2010, 53, 2719–2740. [PubMed: 20131845]
- (43). Lefebvre M; Marchand M; Horowitz JM; Torres G Detection of Fluoxetine in Brain, Blood, Liver and Hair of Rats Using Gas Chromatography-mass Spectrometry. *Life Sci* 1999, 64, 805–811. [PubMed: 10075113]
- (44). McMurray KMJ; Distler MG; Sidhu PS; Cook JM; Arnold LA; Palmer AA; Plant LD Glo1 Inhibitors for Neuropsychiatric and Anti-epileptic Drug Development. *Biochem. Soc. Trans* 2014, 42, 461–467. [PubMed: 24646261]
- (45). Wu Z; Fu Y; Yang Y; Huang C; Zheng C; Guo Z; Yang Z; Chen X; Zhu J; Wang J; Li X; Chen L; Zhou W; Chen Y; Wang J; Yang Y; Jiang M; Chen S; Lv A; Liu J; Li Y; Sun S; Wang Z; Xiao W; Wang Y Gating TrkB Switch by Methylglyoxal Enables GLO1 as a Target for Depression. *bioRxiv* 2018, DOI: 10.1101/435867.
- (46). Jiao J; Nitzke AM; Doukas DG; Seiglie MP; Dulawa SC Antidepressant Response to Chronic Citalopram Treatment in Eight Inbred Mouse Strains. *Psychopharmacology (Berl)* 2011, 213, 509–520. [PubMed: 21181117]
- (47). McMurray KMJ; Du X; Brownlee M; Palmer AA Neuronal Overexpression of Glo1 or Amygdalar Microinjection of Methylglyoxal is Sufficient to Regulate Anxiety-like Behavior in Mice. *Behav. Brain Res* 2016, 15, 119–123.



Scheme 1.
Synthesis disubstituted sulfonamide quinoline derivatives.

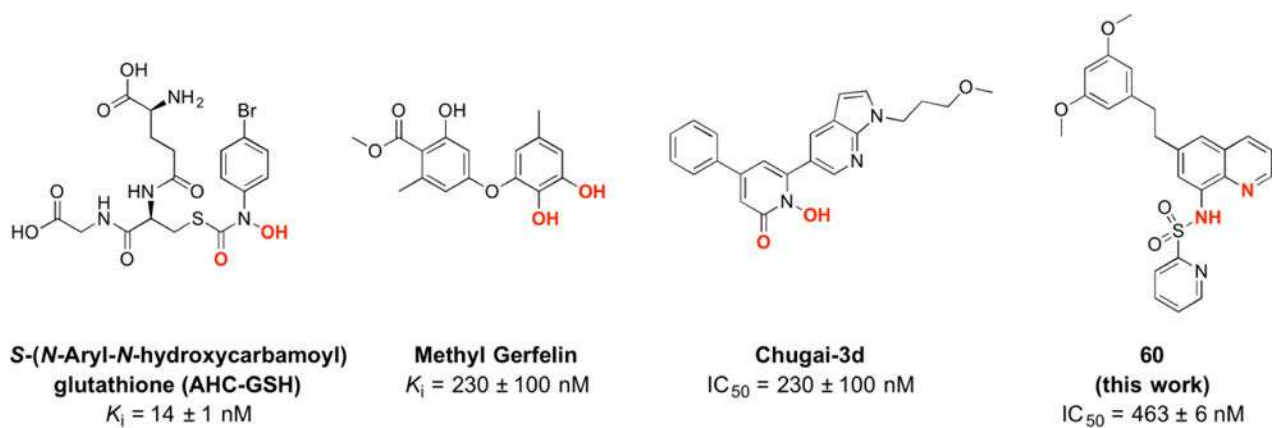


Figure 1. Molecular structures of previously reported GLO1 inhibitors with corresponding K_i or IC_{50} values shown against human GLO1. Metal binding atoms of the MBP are highlighted in bold red.

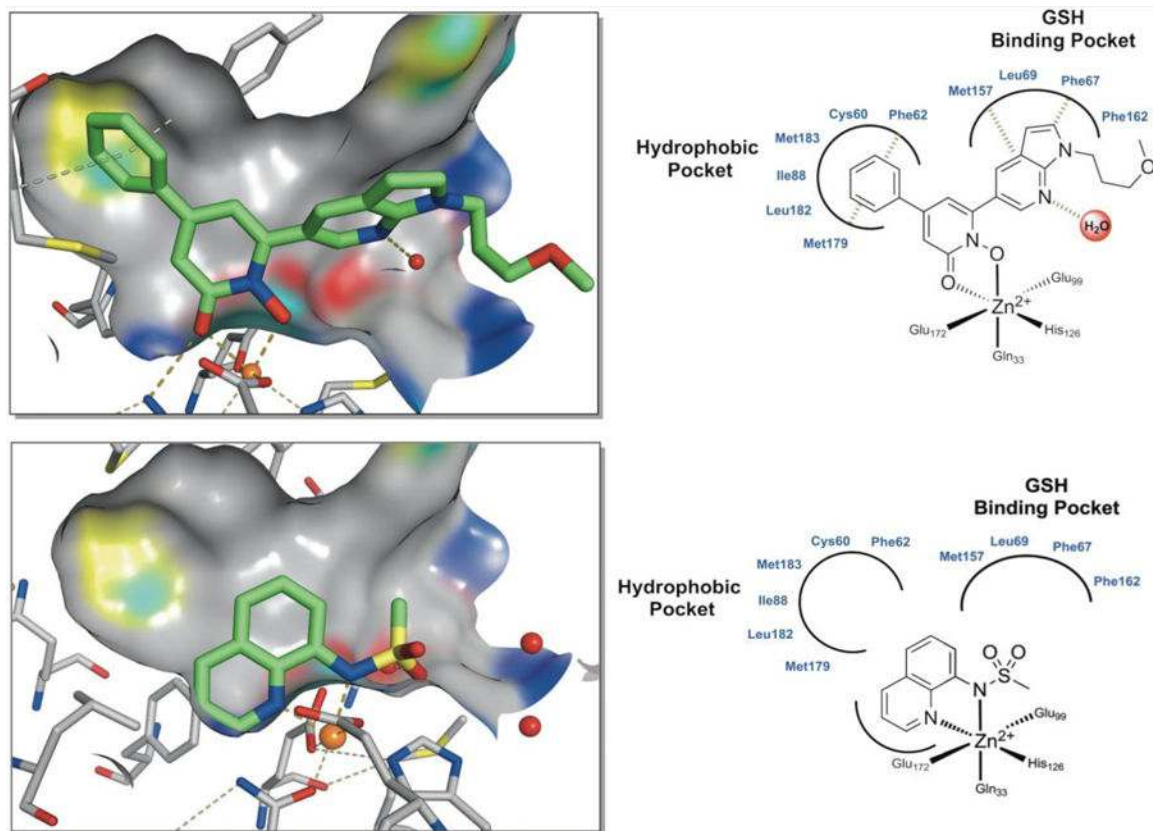


Figure 2.

Top: Structure of **Chugai-3d** bound to the Zn^{2+} ion in the active the GLO1 active site (PDB 3VW9). *Bottom:* Superposition of **8-MSQ** using the structure of the donor atoms of **Chugai-3d** as a guide. For both compounds, an illustration of the interactions is provided (*right*) along with an image of the structure (*left*) with active site surface in gray, the Zn^{2+} ion as an orange sphere, and water molecules as red spheres.

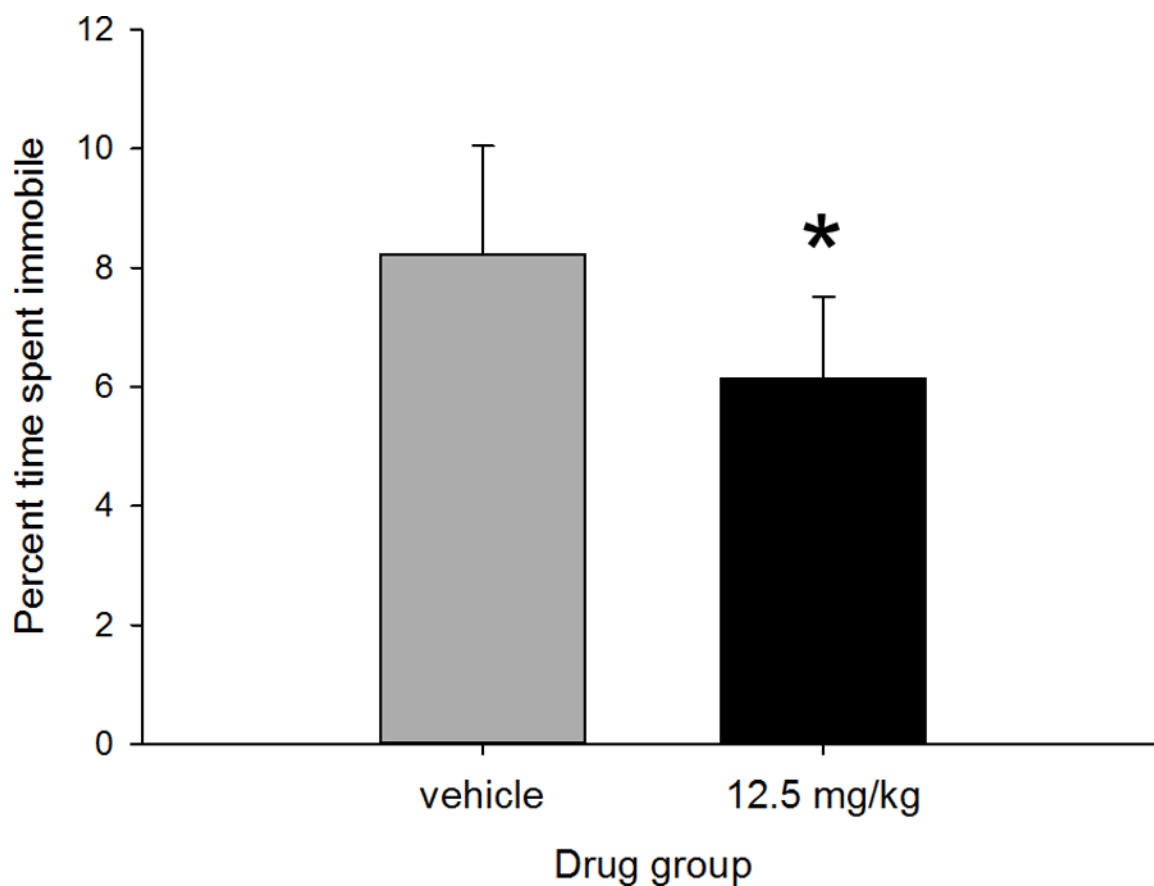


Figure 3.

Administration of compound **60** at 120 min before behavioral testing in the FST produced a significant decrease in the time spent immobile compared to vehicle treated controls (ANOVA; $F_{1,14}=5.06$, $p=0.041$). There were no main effects of sex or test order, and no significant interactions ($F_{1,14} \leq 3.48$, $p>0.05$). There was no effect of drug treatment on locomotor activity ($F_{1,21}=0.052$, $p>0.05$; data not shown), indicating that our results were not confounded by hypo- or hyper-locomotion.

Table 1.

8-MSQ derivatives used to obtain a rudimentary SAR. All IC₅₀ values listed are in μM.

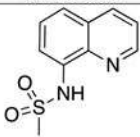
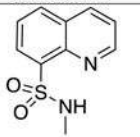
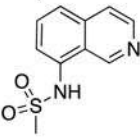
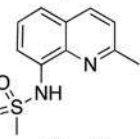
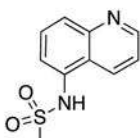
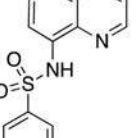
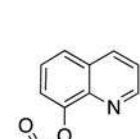
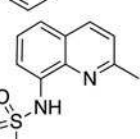
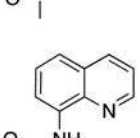
Compound	Structure	IC ₅₀	Compound	Structure	IC ₅₀
8-MSQ		18.5±0.5	6		>200
2		>200	7		43.0±0.2
3		>200	8		8.5±1.2
4		>200	9		14.5± 1.7
5		>200			

Table 2.

8-MSQ fragment derivatives at the 8-position. All IC₅₀ values listed are in μM.

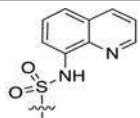
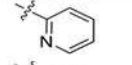

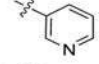
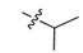
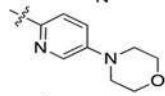

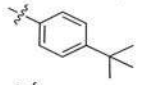
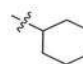
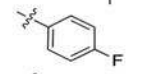
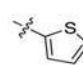
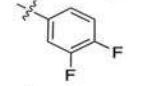
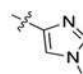
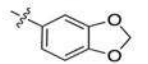
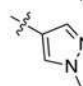
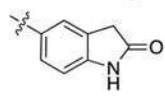
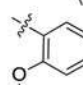
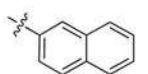
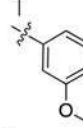
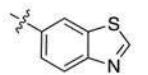
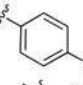
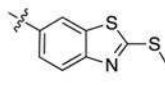
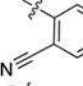
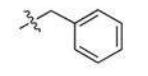
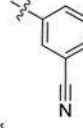
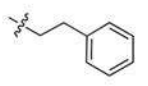
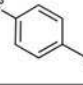
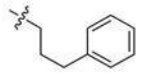
Compound	Structure	IC ₅₀	Compound	Structure	IC ₅₀
8-MSQ		18.5 ± 0.5	23		1.3±0.2
10		>20	24		11.2±2.5
11		>20	25		>20
12		>20	26		4.2±2.2
13		>20	27		7.5±0.7
14		4.9±1.5	28		5.7±2.3
15		5.5±3.7	29		6.1±0.1
16		>20	30		6.6±0.4
17		>20	31		3.6±1.1
18		6.9±0.4	32		3.9±0.1
19		7.0±1.4	33		3.9± 0.1
20		>20	34		7.6±1.0
21		7.3±0.2	35		8.7±0.4
22		6.6±1.2	36		4.6±0.6

Table 3.

8-MSQ fragment derivatives at the 5-position. All IC_{50} values listed are in μM .

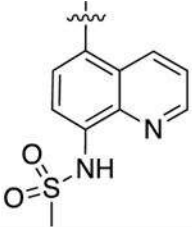

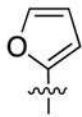
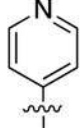

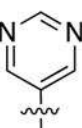
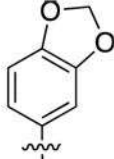
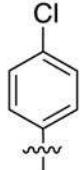
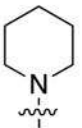
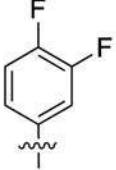
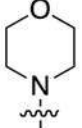

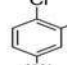
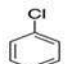
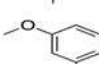
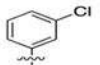
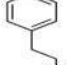
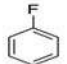
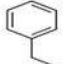
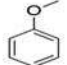
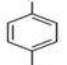
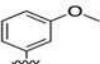
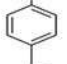
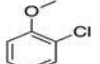
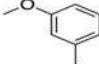
Compound	Structure	IC_{50}	Compound	Structure	IC_{50}
					
37		11.5±1.3	42		11.9±0.1
38		>20	43		15.4±0.2
39		>20	44		11.2±1.9
40		6.2±0.9	45		>100
41		13.9±0.3	46		>100

Table 4.

8-MSQ derivatives with two substituents. All IC₅₀ values listed are in μM.

Cmpd	Position	Structure	IC ₅₀	Cmpd	Position	Structure	IC ₅₀
47	5		0.50±0.04	54	5		0.54±0.21
48	5		0.48±0.01	55	5		1.19±0.62
49	5		0.37±0.02	56	5		0.79±0.13
50	5		0.72±0.01	57	6		1.21±0.08
51	5		0.64±0.10	58	5		0.79±0.33
52	5		1.04±0.26	59	6		1.32±0.01
53	5		0.59±0.15	60	6		0.46±0.01